ACS OMEGA

Open Access

http://pubs.acs.org/journal/acsodf

Review

Recent Progress of High Voltage Spinel $LiMn_{1.5}Ni_{0.5}O_4$ Cathode Material for Lithium-Ion Battery: Surface Modification, Doping, Electrolyte, and Oxygen Deficiency

Seokyoung Choi, Wuliang Feng, and Yongyao Xia*

Cite This: *ACS Omega* 2024, 9, 18688−18708

Read Online

ACCESS | Metrics & More | Article Recommendations

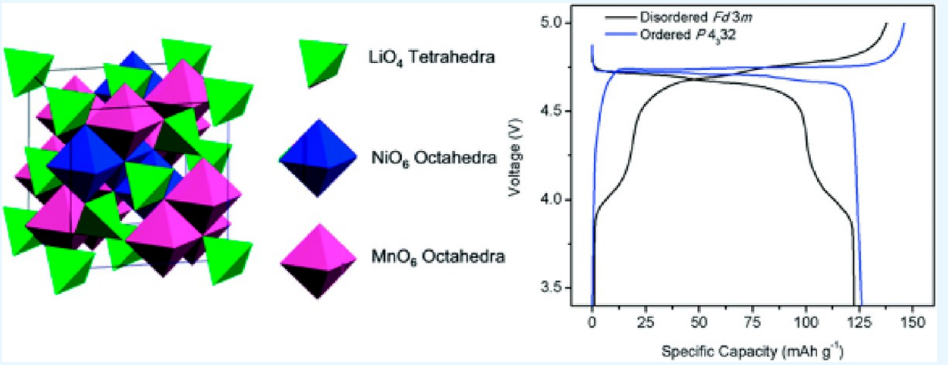

ABSTRACT: High voltage spinel $LiMn_{1.5}Ni_{0.5}O_4$ (LMNO) is a promising energy storage material for the next generation lithium batteries with high energy densities. However, due to the major controversies in synthesis, structure, and interfacial properties of LMNO, its unsatisfactory performance is still a challenge hindering the technology's practical applications. Herein, this paper provides general characteristics of $LiMn_{1.5}Ni_{0.5}O_4$ such as spinel structure, electrochemical properties, and phase transition. In addition, factors such as electrolyte decomposition and morphology of LMNO that influence the electrochemical performances of LMNO are introduced. The strategies that enhance the electrochemical performances including coating, doping, electrolytes, and oxygen deficiency are comprehensively discussed. Through the discussion of the present research status and presentation of our perspectives on future development, we provide the rational design of LMNO in realizing lithium-ion batteries with improved electrochemical performances.

1. INTRODUCTION

Renewable electricity has received great attention due to the lack of traditional fossil fuels and the need to preserve the environment.[1] In the past few decades, there has been immense research and progress in developing sustainable energy, with increasing demands for eco-friendly energy storage systems (ESSs). Among these energy storage methods, electrochemical energy storage devices have come to the fore due to their convenience and energy storage performance.[2,3] Currently, lithium-ion batteries (LIBs) are widely used in a variety of applications, including electric devices, electric vehicles (EVs), and grid energy storage systems.[4−6]

Lithium-ion batteries (LIBs) have gained interest due to their high energy and power densities. So far, various types of oxide cathode materials have been investigated, which all exhibit different characteristics.[7,8] Generally, there are three types of structure with different oxide cathodes: layered ($LiMO_2$, M = metal element), spinel (LiM_2O_4), and olivine structure ($LiMPO_4$). The layered structure, $LiCoO_2$ (LCO) has a theoretical specific capacity of 274 mAh g^{-1}, high theoretical volumetric capacity of 1363 mAh cm^{-3}, low self-discharge, and high discharge voltage. However, its high cost, low thermal stability, and fast capacity fade at high current rates are major limitations.[9] $LiNiO_2$ (LNO) has similar theoretical capacity to LCO, but its thermal stability and blocking of lithium diffusion pathways are major limitations.[10] Spinel structure, $LiMn_2O_4$ (LMO), has a theoretical specific capacity of 147 mAh g^{-1} and has the advantage of lower cost and safety compared to LCO and LNO.[11] Olivine structure, $LiFePO_4$ (LFP), is famous for its high power capability, good safety features, no thermal runaway, and chemical stability with

Received: November 15, 2023
Revised: February 17, 2024
Accepted: February 27, 2024
Published: April 21, 2024

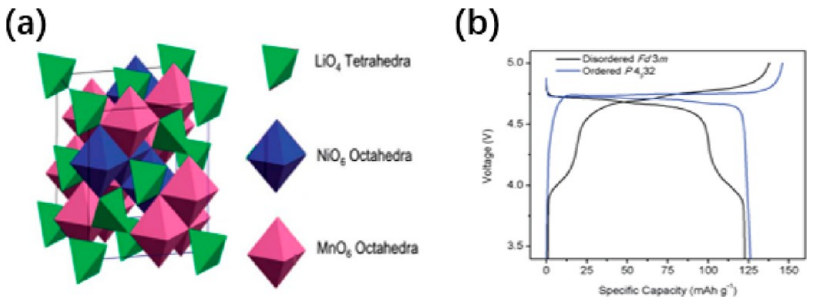

Figure 1. (a) Crystal structure of LMNO and (b) electrochemical charge and discharge profiles for disordered and ordered LMNO structures, reprinted with permission from ref 41. Copyright 2014 Royal Society of Chemistry.

a capacity of 170 mAh g^{-1}.[12] $LiMnPO_4$ (LMP) is a favorable cathode candidate for its high energy density, low toxicity, safe operation, low-performance cost, and adequate thermal electrochemical stability with high redox voltage (4.4 V versus Li^+/Li).[13] Among these structures, spinel structure $LiMn_{1.5}Ni_{0.5}O_4$ (LMNO) has been considered as one of the most promising cathode materials that not only operates at high voltage (4.7 V vs Li/Li^+) but also has a theoretical capacity of 147 mAh g^{-1}, which is 25% higher than spinel $LiMn_2O_4$ structure. Additionally, its energy density (658 Wh kg^{-1}, specific energy density = specific capacity * average operating voltage) is higher than other cathode materials such as $LiCoO_2$ (518Wh kg^{-1}), $LiMn_2O_4$ (440Wh kg^{-1}), $LiFePO_4$ (591Wh kg^{-1}).[14] In addition, several anode materials have been paired with LMNO to study the full cell characteristics.[15−18] Among these materials, $Li_4Ti_5O_{12}$ (LTO), operating at 1.5 V, has gained interest because when it is paired with LMNO cathode, it exhibits a safer and higher power battery with superior electrochemical performance at a voltage window of 3.2 V.[17,19−21] Likewise, in recent years, optimization of LMNO has been studied, such as defect studies by using density functional theory (DFT) to understand the structure of ordered ($P4_332$) and disordered ($Fd\bar{3}m$) phase. These studies focus on understanding the effects of defects on the ordered and disordered phases.[22−24] Moreover, LMNO has the advantages of being inexpensive, easy to synthesize, and having 3D spinel structures that allow rapid Li-ion diffusion.[25,26]

Despite these attractive properties, there are some bottlenecks that hinder the industrialization of LMNO. These limitations mainly arise from the incompatibility of the electrolyte with cathode materials. Because of operating at high redox voltage (~4.9 V), carbonate compounds in the electrolyte decompose and make byproducts, which in turn form a cathode-solid electrolyte interphase (CEI). Creating a continuous CEI layer results in severe polarization and negatively affects electrochemical performance. In addition, Mn dissolution during electrochemical cycling and the formation of impurity (NiO, $Li_xNi_{1-x}O$) phases are also one of the main problems. These disadvantages lead to the continuous growth of CEI, oxygen deficiencies in high temperature, and structure instabilities, which increase the polarization and expedite capacity decay.[5,27] When it comes to full cell, optimization of cell design including choice of electrolyte and anode material needs to be considered.

Tremendous strategies have been developed to deal with the aforementioned bottlenecks. For example, researchers have studied which phase of LMNO exhibits different characteristics. When it is F-type, it helps to exhibit better structural reversibility during both lithiation and delithiation, but it exhibits poor cycling performances due to Jahn−Teller distortion, which induces Mn dissolution into the electrolyte.[28] Also, using surface modification methods are being investigated in which coating acts as a protective layer for high voltage working potential electrodes, which reduces the capacity losses and increases the cycle life.[29] In terms of applying dopant, it helps to increase the structural stability of the LNMO lattice.[30] Moreover, integrating electrolyte additives to prevent undesired side reaction and avoiding the dissolution of transitional metal ions that reduce capacity fading[31,32] and oxygen controlling with temperature that prevents LMNO from structural degradation and enhances the capacity are being investigated.[14,33]

Herein, the purpose of this Review is to comprehensively summarize four aspects to improve the electrochemical performance of LMNO cathode materials: (i) effects of coating, (ii) effects of doping, (iii) effects of electrolyte, and (iv) oxygen deficiency. Detailed information about the factors that affect electrochemical performance of LMNO is provided and help improving strategies that have great potential to be useful for further commercialization will also be proposed. Furthermore, conclusion and perspectives are listed for the possible solutions that are valuable to designing a practicable battery.

2. STRUCTURE OF $LIMN_{1.5}NI_{0.5}O_4$

Knowing the spinel structure of LMNO (Figure 1a) is critical in enhancing electrochemical performances. Due to the influence of ordering Ni and Mn at two octahedral sites, LMNO has two different structures: ordered and disordered. In the stoichiometric ordered ($P4_332$) phases, Li is in 8c sites, Ni in 4a sites, Mn in 12d sites, and O in 8c and 24e sites. In ordered ($P4_332$) phase, Mn and Ni are ordered regularly. On the other hand, in the nonstoichiometric disordered ($Fd\bar{3}m$) phases, Li is on 8a sites, Ni and Mn were randomly distributed on 16d sites, and O is on 32e sites.[34] In the ordered phase, the ordering of Ni and Mn exists without Mn^{3+} ions owing to annealing process below 700 °C that leads to the ordering of Ni and Mn on two distinct octahedral sites and the oxidation of Mn^{3+} ions into Mn^{4+} ions. In contrast, the disordered spinel shows different features that include the disordering of Ni and Mn and the presence of Mn^{3+} ions. The correlation of the disordering of Ni and Mn with the existing of Mn^{3+} ions is because of the synthesis conditions, such as the sintering temperature, postannealing and speed of cooling.[35] In addition, a superlattice can be seen only at the ordered phase, which can be detected by X-ray diffraction (XRD) and Raman spectrum.[36,37] In the XRD, two small peaks are observable at $P4_332$ phase, while it is absent at $Fd\bar{3}m$ phase. This structure

https://doi.org/10.1021/acsomega.3c09101
ACS Omega 2024, 9, 18688−18708

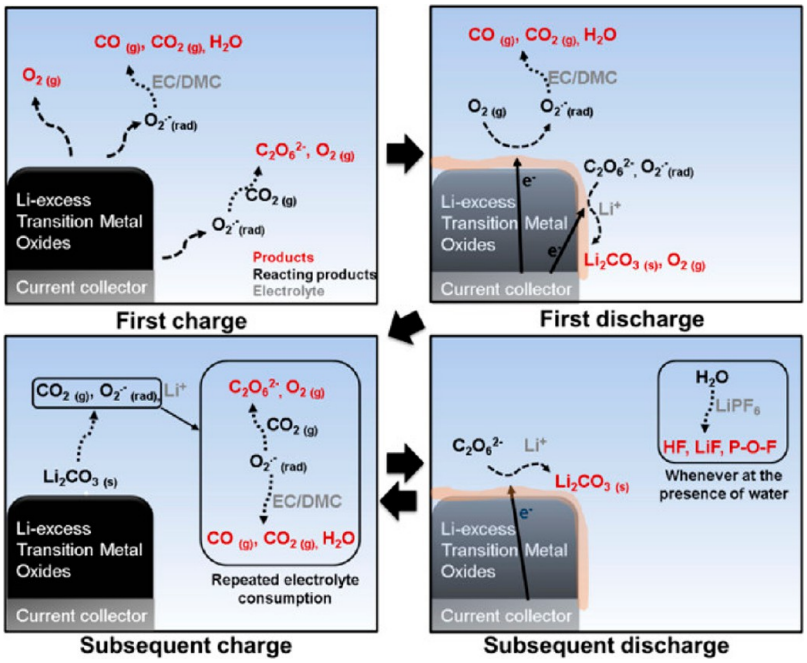

Figure 2. Electrolyte decomposition reactions that occur at high voltage lithium-excess metal oxides, reprinted with permission from ref 46. Copyright 2012 American Chemical Society.

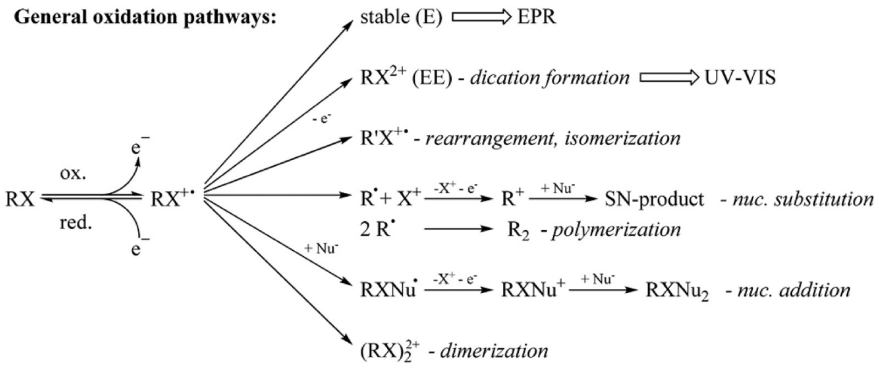

Figure 3. General oxidation pathways for organic species (RX), reprinted with permission from ref 44. Copyright 2022 Wiley-VCH.

difference is also detectable through Raman spectrum, showing more peaks are observable at $P4_332$ phase. As shown in Figure 1b, during the charge/discharge process, when LMNO possesses a superlattice ($P4_332$ phase), two plateau are present at 4 V (Mn redox) and 4.7 V (Ni redox). On the other hand, at $Fd\bar{3}m$ phase, only one peak is observable at 4.7 V (Ni redox).

It has been reported that the electrochemical performance of disordered spinel is better than ordered spinel at high current densities, and its electrochemical performance of LMNO is closely related to structure.[35,38] The presence of Mn^{3+} ions in the spinel plays an important role in the spinel. The impurity of $Li_xNi_{1-x}O$ that reduces the capacity accompanies the disordered formation. In order to maintain charge neutrality in disordered spinel, inactive Mn^{4+} ions are reduced to Mn^{3+} ions.[38] Mn^{3+} ions can increase the electronic conductivity in the disordered spinel, so that Mn^{3+} can improve electrochemical performance. However, existing Mn^{3+} can worsen the electrochemical performances of LMNO due to transforming into Mn^{2+} ions through disproportion reaction, and these Mn^{2+} ions are easily dissolved into electrolyte at high operating temperature and potential.[39] As a result, the presence of Mn^{3+} can also negatively influence the electrochemical performances such as shortening cycle life. Furthermore, disordering Ni and Mn sites in disordered spinel also affect electrochemical performance. Delithiation appears during phase transformation from $P4_332$ structure to structure and leads to disordering Ni and Mn sites.[40] Likewise, understanding the correlation between structure and property relationship is essential to increase electrochemical performances of LMNO.

3. FACTORS AFFECTING ELECTROCHEMICAL PERFORMANCES OF $LiMN_{1.5}NI_{0.5}O_4$

$LiMn_{1.5}Ni_{0.5}O_4$ has a theoretical capacity of 147 mAh g^{-1} due to redox reaction of intercalation of one Li-ion per formula unit owing to the oxidation of Ni^{2+}/Ni^{4+} at around 4.7 V. In ordered $P4_332$ phase only one plateau can be seen in around 4 V that shows absence of Mn^{3+}. However, in disordered, there are two plateaus which are corresponding to the Ni^{2+}/N^{3+} and Ni^{3+}/Ni^{4+} redox reaction around 4.7 V and Mn^{4+}/Mn^{3+} redox reaction at 4 V.[29,41] As mentioned earlier, due to unwanted side reactions and dissolution of Mn ions, many investigations have been conducted in electrolyte decomposition, oxygen deficiency, morphology and phase transition.

https://doi.org/10.1021/acsomega.3c09101
ACS Omega 2024, 9, 18688−18708

Table 1. Electrolytes Used in LMNO

Cell configuration	Electrolyte compositions	Remarks	ref
LMNO/Li	1 M LiPF6 in EC/EMC (3:7) + 1 wt % HFiP		47
	LAGP	solid electrolyte	48
	40PIL-IL (1 M LIFSI in $PYR_{13}FSI$)	solid electrolyte	56
	$Li_{6.4}La_3Zr_{1.4}Ta_{0.6}O_{12}$ (LLZTO)	solid electrolyte	57
	1.3 M $LiPF_6$ in EC/EMC/DEC (3:2:5)		58
	1 M $LiPF_6$ in EC/DEC (3:7) + ETFEC		49
	1 M $LiPF_6$ in EC/EMC (3:7) + 0.1 wt % TPFPS		50
	1 M $LiPF_6$ in EC/EMC (3:7) + 1 wt % DMMP		51
	1 M $LiPF_6$ in EC/EMC (3:7) + 2.5 wt % LiBOB		59
	1 M $LiPF_6$ in EC/DMC/DEC (1:1:1)		60
	1 M $LiPF_6$ in EC/DEC/DMC (1:1:1) + 1 wt % THB		52
	1 M $LiPF_6$ in EC/DEC (1:1) + PAMM		53
LMNO/graphite	1.2 M $LiPF_6$ in EC/EMC (3:7) + 0.1 wt % DMF-SO3		61
	1.2 M $LiPF_6$ in EC/EMC (3:7) + lithium borate	4 types of lithium borate	54
	1 M $LiPF_6$ in FEC/F-EMC/F-EPE (3:5:2)		62
	1 M $LiPF_6$ in EC/EMC/DMC (3:4:3) + 1 wt % TMSP		63
	1.2 M $LiPF_6$ in EC/EMC (3:7) + 0.5 wt % LiCDMB		64
LMNO/$Li_4Ti_5O_{12}$ (LTO)	1 M LiPF6 in EC/DEC (1:2) + 1 wt % LiO-t- C_4F_9 and $Al(HFiP)_3$		55

3.1. Electrolyte Decomposition. It is critical to have appropriate electrolyte with high stability especially in high voltage LMNO cathode materials to deliver full capacity and for long cycle life. Normally, conventional electrolytes composed of $LiPF_6$ salt dissolved in organic carbonate esters such as ethylene carbonate (EC) mix with dimethyl carbonate (DMC) and/or diethyl carbonate (DEC) and/or ethyl methyl carbonate (EMC) are used in LIBs. However, conventional electrolytes have redox reaction which generates acidic species (HF or PF_5) from the decomposition of $LiPF_6$ (Figure 2).[29] In general, the surface film of Li_2CO_3 or LiOH covers the cathode materials, which is formed by reaction of metal oxides with Co_2 and H_2O during the cycle.[42,43] Li_2CO_3 existing on the surface is originated from incomplete conversion of the carbonate precursors.[44] This Li_2CO_3 reacts with electrolyte conducting salts like $LiPF_6$ and $LiBF_4$ and cause the decomposition of electrolyte.[45]

In terms of decomposition of electrolyte, there are three types of reaction pathways: (i) chemical (non-Faradaic) reduction and oxidation, (ii) electrochemical (Faradaic) reduction and oxidation, and (iii) nonredox reactions. (Figure 3) Through these reactions, it can influence on forming interphase layer. In high voltage cell, LMNO, when chemical oxidation is dominant decomposition process, it affects the surface reactivity of positive electrode and electrolyte reaction.[44]

To protect the electrode surface, there has been extensive research and development on electrolytes which also enhance the electronic performances on liquid, solid, and polymer electrolytes. In consequence, it is undeniable that electrolyte plays critical role in batteries and affects electrochemical performances. Electrolytes used in LMNO are shown in Table 1.

Cresce et al. studied highly fluorinated phosphate triester based additive electrolyte. This additive improved anodic stability and provided protective SEI chemistry on graphite anode.[47] Robinson et al. investigated lithium-ion battery with using solid state electrolytes $Li_{1+x}Al_xGe_{2-x}(PO_4)_3$ (LAGP). Despite resulted in good mechanical connection with materials while sintering, Li/LAGP/LMNO exhibited low capacity and high voltage reaction was not reversible on discharge.[48] Zheng et al. investigated ethyl-(2,2,2-trifluoroethyl) carbonate (ETFEC) additive with different ratio. Adding ETFEC as an additive can improve cycle performance, owing to high stability of ETFEC which prevents large oxidation between electrode and electrolyte, especially at high temperature.[49] Lee et al. employed tris(pentafluorophenyl)silane (TPFPS) as an electrolyte additive. This additive showed better Coulombic efficiency compared to TPFPS free electrolyte due to stability to migrate the electrolyte decomposition on the LMNO cathode.[50] Xu et al. investigated the effect of dimethyl methylphosphonate (DMMP) additive. Addition of DMMP exhibited better capacity retention, owing to suppress the decomposition between electrode which contribute to improve electrochemical performances.[51] Perea et al. studied the effect of adding additive 1,3,5-trihydroxybenzene (THB). Addition of THB improved the capacity retention by inhibiting electrolyte decomposition on the cathode surface.[52] A cross-linking polymer network of acrylic anhydride-2-methyl-acrylic acid-2-oxirane-ethyl ester-methyl methacrylate (PAMM) based electrolyte is introduced by Ma et al. Performances such as electrochemical stability, mechanical strength, flame resistance, interphase compatibility, and suppressing Mn dissolution, are increased by using PAAM based electrolyte.[53] Four types of lithium borate electrolyte (LFPTB, LPTB, LTSTB, LPrTB) is presented by Xu et al. Among those, lithium 4-pyridyl trimethyl borate (LPTB) exhibited the best performance improvement. LPTB enables generation of a cathode passivation film and acts as a functional group delivery which results in improved capacity retention and efficiency.[54] Two additives, LiO-*t*-C_4F_9 and $Al(HFiP)_3$, to the electrolyte are studied in LMNO/LTO cell. LiO-*t*-C_4F_9 additive improves capacity retention by increasing electrolyte oxidation at the cathode. For the $Al(HFiP)_3$ additive, it reduces parasitic reaction at LMNO electrode but does not affect capacity retention.[55]

3.2. Oxygen Deficiency. Oxygen deficiency is one of the key factors that should be considered when using LMNO as cathode material. As aforementioned, LMNO oxygen deficiency occurs during structural change from low temperature (below 700 °C) ordered structure, $P4_332$ to high temperature (over 700 °C) disordered structure, $Fd\bar{3}m$ phase.

https://doi.org/10.1021/acsomega.3c09101
ACS Omega 2024, 9, 18688−18708

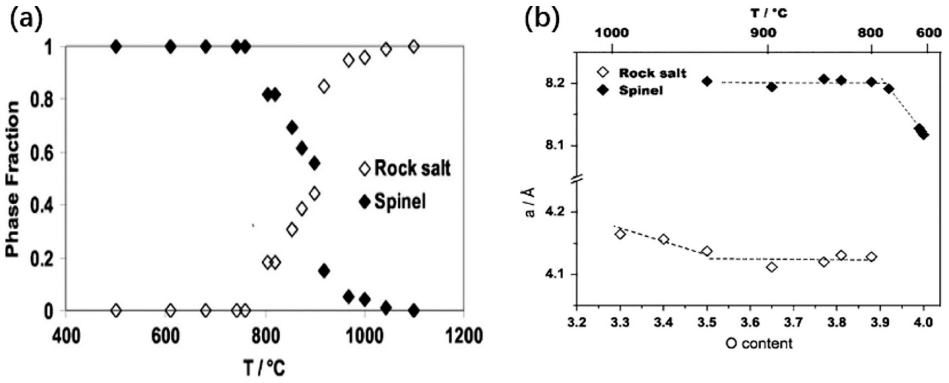

Figure 4. (a) Correlation between phase fraction and temperature and (b) correlation between phases and oxygen content, reprinted with permission from ref 66. Copyright 2008 Electrochemical Society.

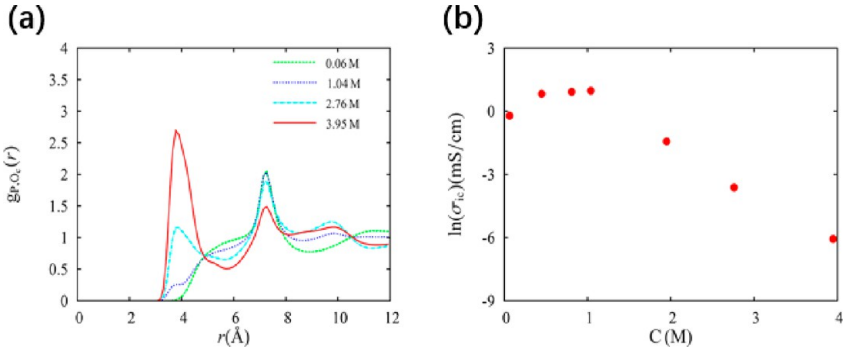

Figure 5. (a) Radical distribution function value and (b) ionic conductivity with different concentrations of $LiPF_6$, reprinted with permission from ref 75. Copyright 2018 American Chemical Society.

This disordered structure is accompanied by a rock salt impurity phase such as Ni_x, $Li_xNi_{1-x}O$, and $(LiNiMn)O_4$ and with oxygen deficiency within the spinel.[65] To be more specific, a correlation between structure and temperature with oxygen content is shown in Figure 4. A temperature below 683 °C shows a single phase; a temperature between 683−805 °C shows a single phase with an increase in unit cell volume; a temperature between 805−950 °C shows two phases coexist; a temperature above 950 °C shows a single cubic rock salt phase.[66] Also, oxygen deficiency in LMNO can be shown as $LiMn_{1.5}Ni_{0.5}O_{4-x}$. When x is below 0.05, it has single spinel phase ($P4_332$); when x is between 0.05 and 0.18, it has a single spinel phase ($Fd\bar{3}m$); when x is between 0.18 and 0.7, it has two phases, spinel phase ($Fd\bar{3}m$) and rock salt phase ($Fm\bar{3}m$); when x is over 0.7, it has two phases, rock salt phase ($Fm\bar{3}m$) and secondary spinel phase ($Fm\bar{3}m$). During this phase transition, oxygen is released from the cathode material, Mn^{4+} changes to Mn^{3+} in order to satisfy the charge balance. Also, as temperature increases, Kunduraci et al. showed that surface area, lattice parameters, and weight loss depend on the temperature.[67]

Oxygen deficiency can also occur through various ways such as delithiation, side reaction of electrolytes. When transitional metal Mn^{3+} changes to Mn^{4+} during the charging process (delithiation), LMNO become more oxidative and releases oxygen.[68] Charging induced oxygen loss is exacerbated when cutoff voltages above 4.4 V are adopted. On the other hand, voltages under 4.3 V results in reduced kinetics of oxygen loss.[33] In the voltage region of 3−4.4 V, delithiation reaction is related to the oxidation of Ni and voltage region around 4.5 V is related to Mn sites during charging.[69] Likewise, voltage plateau ∼4.5 V is attributed to an oxygen loss and structural change. This voltage plateau does not show up in the layered cathodes other than LMR cathodes, primarily because they do not have such pronounced oxygen loss in the first cycle.

Unwanted side reaction from the electrolytes can cause the oxygen loss. Due to oxygen's high potential property, oxygen from cathode is highly oxidative and the reduction of oxygen forms a free oxygen radical in the electrolyte as shown in Figure 2.[70,71] These oxygen radicals yield a byproduct such as H_2O and CO_2. The existence of H_2O can lead to the production of impurities of Li_2O or by diffusion of Li and O from the cathode and affects electrochemical performances by producing LiF.[33,72] In terms of CO_2, it reacts with Li_2O to form Li_2CO_3. And Li_2CO_3 along with LiF can form a SEI layer coated on the surface on the particle, which decreases the conductivity.[46]

In order to compensate for this oxygen loss from the particle, surface coating, increasing lithium content, and controlling cooling rate have been used. As mentioned above, oxygen loss and structural degradation occur on the surface of the particle. Therefore, surface coating acts as a protection barrier that induces an improvement electrochemical performance in LIBs.[73] In terms of doping, the latest report was shown by Liang et al., who presented new orbital hybridization.[74] They found Ge (at 16c site) with valence state of +3 in 4s orbital that enables to interact with oxygen electrons in the 2p orbital. This 4p-2s orbital hybridization with Ge gives LMNO enhanced stability for the metal oxygen framework. Also, it contributes to stable thin CEI and prevents LMNO from structural collapse.

https://doi.org/10.1021/acsomega.3c09101
ACS Omega 2024, 9, 18688−18708

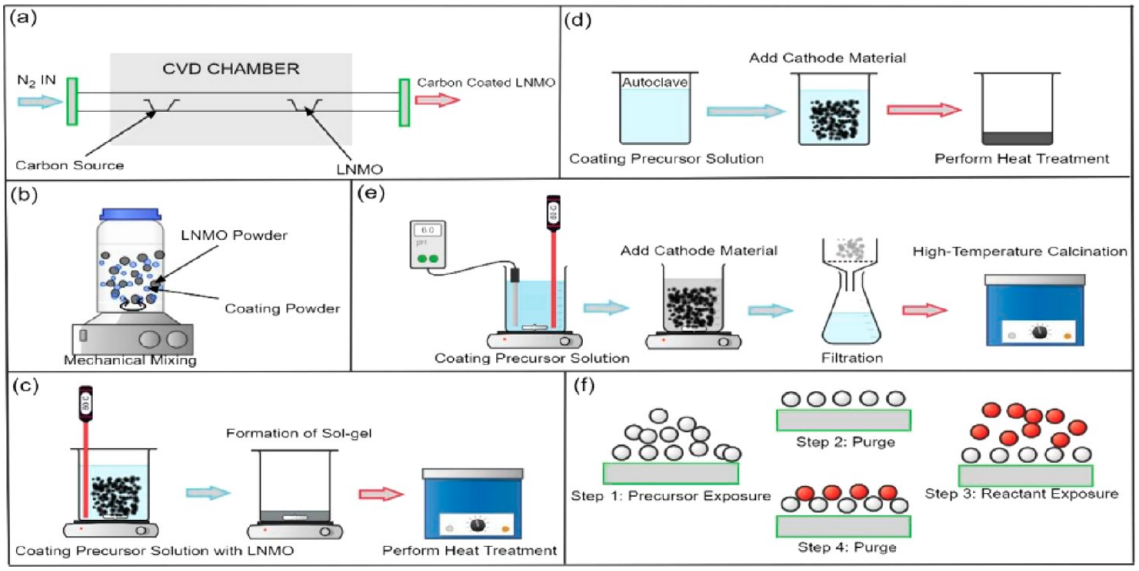

Figure 6. Coating methods (a) CVD, (b) Ball mill, (c) Sol−gel, (d) Solvothermal, (e) Coprecipitation, (f) ALD methods, reprinted with permission from ref 28 Copyright 2022 Elsevier.

As mentioned above, oxygen from the cathode can react with Li, forming Li_2O. The equation will be $2Li^+ + O^{2-} = Li_2O$, and from this equation, the equilibrium K_c will be $K_c = [Li_2O]/([Li^+]^2 * [O^{2-}])$. Hence, increasing the lithium salt will reduces the concentration of oxygen radical. Therefore, excess lithium will reduce the migration of lattice oxygen from the cathode into the electrolyte.[33] However, when the concentration of $LiPF_6$ increases, there are both advantages and disadvantages. For the advantages, when the concentration of $LiPF_6$ increases, the value of radical distribution function increases which improves stability and reduces the interaction with electrode and oxygen loss (Figure 5a). On the other hand, for the disadvantages, when the concentration of $LiPF_6$ increases, ionic conductivity decreases due to a decrease of diffusivity (Figure 5b).[75]

In terms of electrochemical performance depending on the temperature, Pasero et al. introduced compared 4 different samples: quenched from 855 °C, 805 °C, 743 °C, HOP (slow cooling under pressure to room temperature). These samples' discharge capacity varies from 120−140 mAh g^{-1}. With increasing quench temperature, the plateau begins to appear at 4 V. Also, HOP sample shows the best capacity retention and sample quenched from 855 °C shows the worst capacity retention.[66] Tong et al. also compared 4 different samples which quenched from 750 °C (S750), 700 °C (S700), 650 °C (S650), and SRT (slow cooling to room temperature). Besides SRT sample (ordered sample), they all exhibits two plateaus at 4 and 4.7 V which corresponds to Mn and Ni redox. Under the rate of 5C, S750 and S700 achieves 80% capacity retention after 1000 cycles, but S650 and SRT retain only 54% and 24% of capacity.[76] Sun et al. heated samples with 5 different temperatures (650 °C, 750 °C, 850 °C, 950 °C, 1000 °C). Samples heated up to 650 and 750 °C (ordered phase) show only one plateau at 4.7 V and the others all exhibit two plateau at 4 and 4.7 V. Discharge capacity of these samples show 125.2, 121.3, 134.5, 126.8, 106 mAh g^{-1}, respectively. They show 86.27, 84, 99.32, 91.76, 88.52% capacity retention from 10th cycle to 50th cycle at 1C.[77]

3.3. Morphology. Different morphology is studied to enhance the electrochemical performances including cycling and rate performances. After been through different approach (synthesis, doping, surface modification, and etc.) morphology changes from spinel structure to different structure. Kebede reported LMO@LMNO having polyhedral morphology which enhanced rate capability. This product shows 123 mAh/g discharge capacity at 0.2C and shows 96.2% retention after 120 cycles.[78] Tong et al. introduced microrods morphology through metal oxalate precursor. The resulting product showed excellent capacity retention up to 20C. Plus LNMO microrods quenched at 700 °C deliver a capacity of 116 mA h g^{-1} even at a discharging rate of 50 C, and the electrode maintains 80% of its capacity after 1000 cycles at 5 C.[76] Karunawan et al. proposed truncated octahedral shape LMNO with plausible crystal growth mechanism via solid state method. The resulting product exhibited 128.53 mAh g^{-1} with high initial Coulombic efficiency (ICE) with superior cycling stability which retained 90.32% after 250 cycles.[79] And the others are mentioned in section 4.

3.4. Phase Transition. Phase transition is also one of the factors that influence electrochemical performances of LMNO. As shown in Figure 1b, two different phases have different capacity. Likewise, knowing a phase transition is one of the key factors to understand the LMNO. Through various studies, it is reported that LMNO has been through different phases: (i) from disordered phase ($Fd\bar{3}m$) to ordered phase ($P4_332$). In this phase transition, there are three characteristics: cationic ordering at 4a and 12d sites, anionic ordering at 8c and 24e sites, and displacement of all atoms; (ii) from spinel ($Fd\bar{3}m$) phase to rock salt ($Fm\bar{3}m$) phase. In this phase transition, one-half of O_2 is released by the spinel to yield the rock salt phase; and (iii) from cubic ($Fd\bar{3}m$) phase to tetragonal $I4_1/$ and spinel structure.

4. METHODS IMPROVING ELECTROCHEMICAL PERFORMANCES OF $LiMn_{1.5}Ni_{0.5}O_4$

As mentioned above, many cathode materials are undergoing different problems. In order to improve electrochemical performances of LMNO, many researchers used different approaches to solve the problems. Generally, three different

https://doi.org/10.1021/acsomega.3c09101
ACS Omega 2024, 9, 18688−18708

Table 2. Characteristic of Different Coatings Using CVD Method

Synthesis Method	Particle size	Lattice constant (Å)	Morphology	Surface Modification	Capacity (mAh g^{-1})/ temperature	Capacity retention (Rate/Cycle)	Remarks	ref
CVD	-	-	truncated octahedron	SnO_2	135 at 0.5C/25 °C	95.21% at 1C/100	-	81
	-	-	spherical	Al	131.6 at - /25 °C	81% at - /400	10 nm Al coated	82

techniques are introduced in this paper: surface modification, doping, and CEI modification.

4.1. Surface Modification. Surface modification has been reported to have advantages of suppressing the side reaction that decreases the overall capacity and cycle ability and dissolution of transition metal ions. The main effects of surface coating can be the following: (i) enables the charge transfer at the surface of the particle, (ii) changes the particle's morphology, (iii) suppresses the metal dissolution and side reaction.[73] Also, it has been found to provide a stable interface between the electrolyte and the active material which derived higher electrochemical performances with various coating methods: Chemical vapor deposition process (CVD), dry coating, atomic layer deposition (ALD), coprecipitation, radio frequency magnetron sputtering, sol−gel, solvothermal (Figure 6).[28]

4.1.1. Chemical Vapor Deposition (CVD). Chemical vapor deposition (CVD) is a coating method that uses chemical reactions at the surface of a heated substrate, with reagents supplied in gas phase precursors. CVD is known to offer an advantage by depending on chemical reactions which allow tunable deposition rates and high quality products.[80]

There are essential sequential phases in every CVD process: reactants are transferred convectively and diffusively from gas inlets to reaction zone, generation of new active species through gas phase chemical process, transportation of starting reactants and their products to the target substrate, chemical/physical adsorption and diffusion of substances on the substrate surface, film formation through surface-catalyzed heterogeneous processes, desorption surface reaction through volatile derivatives, byproducts are transferred convectively and diffusively in the reaction away from the reaction zone.[28] Characteristics of different coatings are shown in Table 2.

Lee et al. used tin oxide by employing electron cyclotron resonance metal−organic chemical vapor deposition to prepare the SnO_2-LMNO cathode. It not only performed with better rate capability at both room temperature and 60 °C, but also effectively suppressed the charge transfer resistance.[81] Sun et al. employed an electron-beam vapor deposition approach to make Al coating on LMNO. Al-LMNO showed low impedance owing to the presence of a conductive Al layer, which performed with better rate capability. They also presented that Al-coated LMNO can be turned to Al^{3+} doped LMNO at high temperature (Figure 7).[82]

4.1.2. Dry Coating. In the dry coating method, larger particles are directly coated using smaller fine particles by external mechanical forces without using any solvents and binders.[83] Larger particles that create engineered particulates with tailored properties can be changed in property or function.[84] It can be considered that the intimate electrode−electrolyte contacts are built by dry coating of the electrode particles with the solid electrolyte particles.[85] Dry coating has the advantage of improving the dispersion and adhesion onto the cohesive particles.[86] Characteristics of different coatings are shown in Table 3.

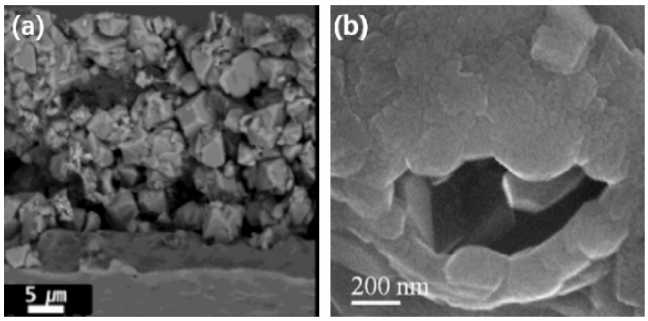

Figure 7. SEM images of (a) SnO_2 coated LMNO, reprinted with permission from ref 81. Copyright 2015 Elsevier. SEM images of (b) Al coated LMNO, reprinted with permission from ref 82. Copyright 2016 Elsevier.

Nisar et al. used ball milling process to coat LMNO with silica nanoparticles. It exhibited better cycle and rate capability with high retention owing to high charge transfer kinetics and low interfacial charge transfer resistance.[87] Cho et al. presented three different coating materials: SiO_2, Al_2O_3, TiO_2, and $MgCO_3$. These coated LMNO exhibited structural stability and suppressed Mn dissolution with high capacity retention.[88] Ben et al. employed Ta_2O_5 as a coating material. Ta_2O_5 coated LMNO exhibited high capacity retention and better cycling performances at room temperature and 55 °C. It has advantage of high resistance against hydrofluoric acid (HF) attack.[89] Chong et at., presented $Li_4P_2O_7$ coated LMNO, which exhibited better rate capability and cycling capability. $Li_4P_2O_7$ coating layer acts as a solid electrolyte or artificial SEI layer that prevents Ni redox couple from decomposing the electrolyte.[90] Yang et al. employed a Cr doped $Li_{0.1}B_{0.967}PO_4$ (LBPO) coated material on LMNO. Cr^{3+} doping reduces NiO impurity and enhances structural stability, and LBPO can enhance Li^+ transference and suppress the unwanted side reaction. Overall, Cr doped $Li_{0.1}B_{0.967}PO_4$ exhibited better cycle stability and rate performances (Figure 8).[91] Liu et al. employed C-$LiFePO_4$ as a coating material on LMNO. C-$LiFePO_4$ coated LMNO exhibited better capacity retention (at high rate) and cyclability in room temperature. This coated LMNO showed high surface conductivity and prevents the reaction that occurs in the electrolyte.[92]

4.1.3. Atomic Layer Deposition (ALD). Atomic layer deposition (ALD) is a self-limiting half reaction that comes along with surface-controlled and iterative monolayer-by-monolayer process relied on two sequential.[94] Most of the ALD processes have binary reaction sequences where two surface reactions occur and deposit a binary compound film. Due to a finite number of surface sites, a finite number of surface species can be deposited.[95] ALD enables the deposition of material precise angstrom-level thickness with excellent consistency and has the advantages in the application of surface coatings on LIB cathode and anode materials.[94] Characteristics of different coatings are shown in Table 4.

https://doi.org/10.1021/acsomega.3c09101
ACS Omega 2024, 9, 18688−18708

Table 3. Characteristic of Different Coatings Using Dry Coating Method

Synthesis method	Particle size	Lattice constant (Å)	Morphology	Surface modification	Capacity (mAh g^{-1})/ temperature	Capacity retention (Rate/Cycle)	Remarks	ref
dry coating	2 μm	-	truncated octahedron	SiO_2	122 at 40C/55 °C	82.4% at 80C/400	1 wt % SiO_2	87
	-	-	truncated octahedron	SiO_2	127.2 at 1C/25 °C	89%% at 1C/100	3 wt % SiO2	88
	-	-	truncated octahedron	Al_2O_3	116.6 at 1C/25 °C	91.5% at 1C/100	3 wt % Al_2O_3	88
	-	-	truncated octahedron	TiO_2	119.9 at 1C/25 °C	91.6% at 1C/100	3 wt % TiO_2	88
	-	-	truncated octahedron	$MgCO_3$	121.2 at 1C/25 °C	95.4% at 1C/100	3 wt % $MgCO_3$	88
	1−2 μm	8.1651	octahedron	Ta_2O_5	131.5 at C/10/55 °C	97% at 0.2C/100	2 wt % Ta_2O_5	89
	1 μm	-	polyhedron	ZrO_2	110 at 40C/25 °C	85.6% at 40C/1200	1 wt % ZrO_2	93
	0.53 μm	-	polyhedron	$Li_4P_2O_7$	123.8 at 0.5C/25 °C	74.3% at 0.5C/893	0.05 mol ratio	90
	100 nm−1 μm	-	octahedron	$Li_{0.1}B_{0.967}PO_4$	137.1 at 1C/25 °C	91.3% at 1C/400	Cr doped	91
	-	-	spherical	C-$LiFePO_4$	82 at 1C/25 °C	74.5% at 1C/140	20 wt % LFP (2 wt % C)	92

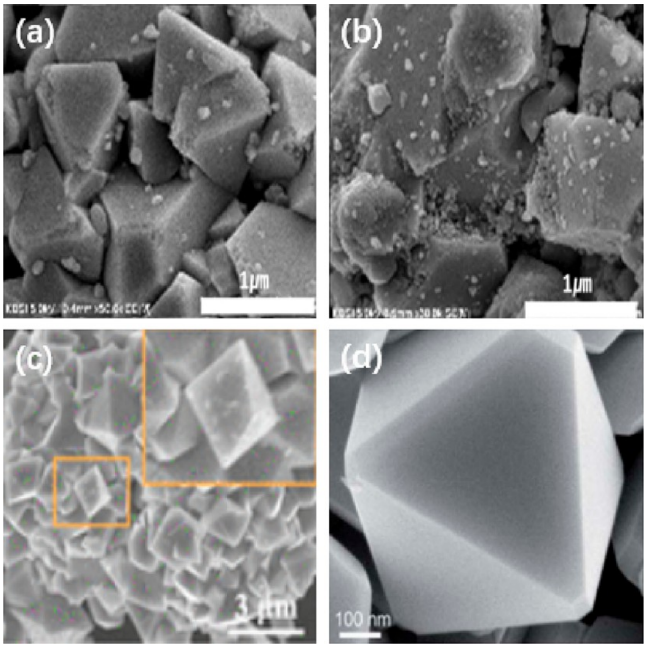

Figure 8. SEM images of (a) $MgCO_3$-LMNO, reprinted with permission from ref 88. (b) Al_2O_3-LMNO (dry coating), reprinted with permission from ref 88. Copyright 2019 Springer Nature. (c) Ta_2O_5-LMNO, reprinted with permission from ref 89. Copyright 2018 American Chemical Society. (d) Cr doped $Li_{0.1}B_{0.967}PO_4$-LMNO, reprinted with permission from ref 91. Copyright 2014 Royal Society of Chemistry.

Cho et al. employed TiO_2 and Al_2O_3 as a thin coating material on LMNO nanowire through ALD synthesis method. This coated LMNO enables decreasing irreversible capacity fade and diminishing the Mn dissolution, which led to acceleration of Li ion migration and reduction in resistance.[96] Song et al. presented Al_2O_3 coated LMNO by ALD process. Al_2O_3 coated LMNO exhibited reduced side reactions involving organic components of the electrolyte decomposition, which results in high capacity retention.[97] Xiao et al. presented ultrathin $FePO_4$ coated LMNO. $FePO_4$ layer acts as Li ions reservoir and active buffer that leads to high capacity. With 10 ALD cycles of $FePO_4$ coated LMNO, there was stabilized capacity retention and suppressed Mn dissolution, along with the advantages on the electron/ion diffusion on the surface.[98] Deng et al. designed a hybrid Li_3PO_4−TiO_2 coated LMNO. The Li_3PO_4−TiO_2 coating layer helps to inhibit the side reactions and enhance interfacial ionic and electronic conductivities. As a result, Li_3PO_4−TiO_2 coated LMNO exhibited improved rate capability and cyclic stability.[99] They also designed $AlPO_4$ coated LMNO, which exhibited a high capacity retention with long cycle life (Figure 9).[100] Park et al. used the $LiAlO_2$ coating material on LMNO with improved electrochemical stability.[101]

4.1.4. Coprecipitation. Coprecipitation is considered an efficient, simple, scalable, and tunable technique.[103] Especially, coprecipitation reaction has been widely used in high volumetric energy-density cathode materials.[104] Usually, there are two main steps using coprecipitation process to synthesize battery active materials. The first step involves formation of

Table 4. Characteristic of Different Coatings Using ALD Method

Synthesis method	Particle size	Lattice constant (Å)	Morphology	Surface modification	Capacity (mAh g^{-1})/ temperature	Capacity retention (Rate/ Cycle)	Remarks	ref
ALD	-	-	nanowire	TiO_2	103.17 at C/7.5/25 °C	-	-	96
	-	-	nanowire	Al_2O_3	105.72 at C/7.5/25 °C	-	-	96
	-	-	-	Al_2O_3	115 at 0.5C/25 °C	92% at 0.5C/200	4 cycles of ALD	97
	-	-	-	Al_2O_3	130 at 0.5C/25 °C	91% at 0.5C/200	-	102
	-	-	-	$FePO_4$	112 at 0.5C/25 °C	91.96% at 0.5C/100	10 cycles of ALD	98
	-	-	-	Li_3PO_4−TiO_2	122 at 0.5C/25 °C	81.2% at 0.5C/300	-	99
	-	-	-	$AlPO_4$	100.6 at 0.5C/25 °C	94% at 0.5C/100	10 cycles of ALD	100
	-	-	-	$LiAlO_2$	92 at C/3/25 °C	-	-	101

https://doi.org/10.1021/acsomega.3c09101
ACS Omega 2024, 9, 18688−18708

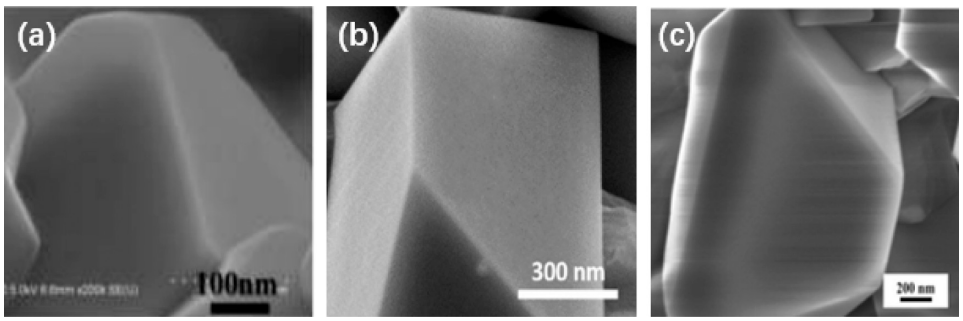

Figure 9. SEM images of (a) $FePO_4$-LMNO, reprinted with permission from ref 98. Copyright 2015 Wiley-VCH. (b) LPO-TiO coated LNMO, reprinted with permission from ref 99. Copyright 2019 Elsevier. (c) ALP −50 coated LMNO, reprinted with permission from ref 100 Copyright 2017 Elsevier.

Table 5. Characteristic of Different Coatings Using Coprecipitation Method

Synthesis method	Particle size	Lattice constant (Å)	Morphology	Surface modification	Capacity ($mAh\ g^{-1}$)/ temperature	Capacity retention (Rate/Cycle)	Remarks	ref
coprecipitation	-	8.174	spherical	CeO_2	138 at 0.1C/25 °C	96.8% at 0.1C/100	1 wt % CeO_2 wrapped in graphene	106
	-	-	octahedron	MoO_3	128 at 0.1C /-	94.6% at 0.1C/100	2 wt % MoO_3	107
	-	-	spherical	FeF_3	132 at C/6/25 °C	100% at -/200	2 wt % FeF_3	108
	10 μm (sphere size)	-	spherical	Fe_2O_3	126 at 1C/25 °C	98.6 at 1C/100	-	110
	700 nm (polygon size)	-	polyhedron	CuO	131.5 at 0.5C/25 °C	96.5% at 0.5C/100	3 wt % CuO	111
	-	-	polyhedron	Co_3O_4	126 at 1C/25 °C	96.8% at 1C/300	5 wt % Co_3O_4	112
	-	-	spherical	Co_3O_4	127.7 at 0.2C/25 °C	81% at 5C/2000	-	113
	-	-	crystalline	ZrO_2	118 at 1C/25 °C	96% at 1C/150	1 wt % ZrO2	109
	-	8.173	spherical	Y_2O_3	127.2 at 2C/55 °C	97.7% at 1C/300	-	114
	-	-	octahedron	RuO_2	131.7 at 0.5C/25 °C	97.7% at 0.5C/100	2 wt % RuO_2	115
	200 nm	8.175	polyhedron	YPO_4	138 at 0.1C/25 °C	77.5% at 0.1C/240	3 wt % YPO_4	116
	300 nm	8.1782	polyhedron	YF_3	108 at 0.1C/25 °C	84% at 0.1C/100	2.8 wt % YF_3	117
	-	-	octahedron	AlF_3	103.6 at 0.1C/25 °C	93.6% at 0.1C/50	1 wt % AlF_3	118
	200 nm	8.1614	polyhedron	MgF_2	115.3 at 0.1C/25 °C	89.9% at 0.1C/100	5 wt % MgF_2	119

particles from a coprecipitation reaction (precursors). These precursors are dried to get rid of residual water or other solvents. And then, the precursor particles are mixed with a lithium source and calcined to produce the final active materials that is used in battery electrodes.[105] There are many factors that can influence the composition and morphology of the particles such as temperature, pH, concentration, stirring rate and mixing method, rate of reactant feed, and the use of additives. Characteristics of different coatings are shown in Table 5.

Qureshi et al. designed CeO_2 coated LMNO wrapped in graphene. CeO_2 coating layer helps to suppress the reaction at the electrolyte/electrode and Mn dissolution. In terms of graphene wrapping, it helps to reduce material aggregation and improves conductivity which results in improvement of electrochemical performances. Overall, this coated LMNO exhibited better cyclability and capacity retention.[106] Wu et al. employed MoO_3 as a coating material. MoO_3 coating layer not only enables to improve the high rate charge/discharge profiles and cycle life but also suppress the side reactions at electrode and in electrolyte. Thus, MoO_3 coated LMNO displayed better cyclic retention and electrochemical performances (Figure 10).[107] Luo et al. used FeF_3 as a coating material on LMNO by precipitation method. FeF_3 coated LMNO displayed enhanced electrochemical properties and thermal stability.[108] Wu et al. designed ZrO_2 and ZrP_2O_7 coated LMNO. ZrO_2 coated LMNO by coprecipitation method, exhibited improved cycling stability with high capacity retention. On the other hand, ZrP_2O_7 coated LMNO by the sol−gel method, exhibited lower capacity retention than ZrO_2 coated LMNO.[109]

4.1.5. Radio Frequency Magnetron Sputtering. Radio frequency (RF) magnetron sputtering is the technique that argon ions are accelerated by radio frequency (RF) electric field in order to hit a target to sputter. It enables to produce even films and has the advantage of low costs, high efficiency, easy control, and high deposition rates.[120] RF sputtering is widely used in thin film of LIBs for surface treatment of active materials, anodes and cathodes, current collectors, and components of battery materials.[121]

4.1.6. Sol−Gel. The sol−gel method is a wet-chemical process that involves the formation of an inorganic colloidal suspension (sol) and gelation of the sol in a continuous liquid phase (gel) to form a three-dimensional network structure.[122] Using the sol−gel method, a solid phase is generated by gelation of a colloidal solution. Then gel is dried to form a "dry gel" (xerogel), and in order to stabilize, densify, and eliminate unreacted organic residues, heat treatment is used.[28] The sol−gel method is well-known as one of the promising thin-film preparation methods, which has been utilized to prepare various kinds of transition metal oxide thin films to construct thick film rechargeable lithium batteries with low cost and high deposition.[123,124] This sol−gel method can provide thin film

https://doi.org/10.1021/acsomega.3c09101
ACS Omega 2024, 9, 18688−18708

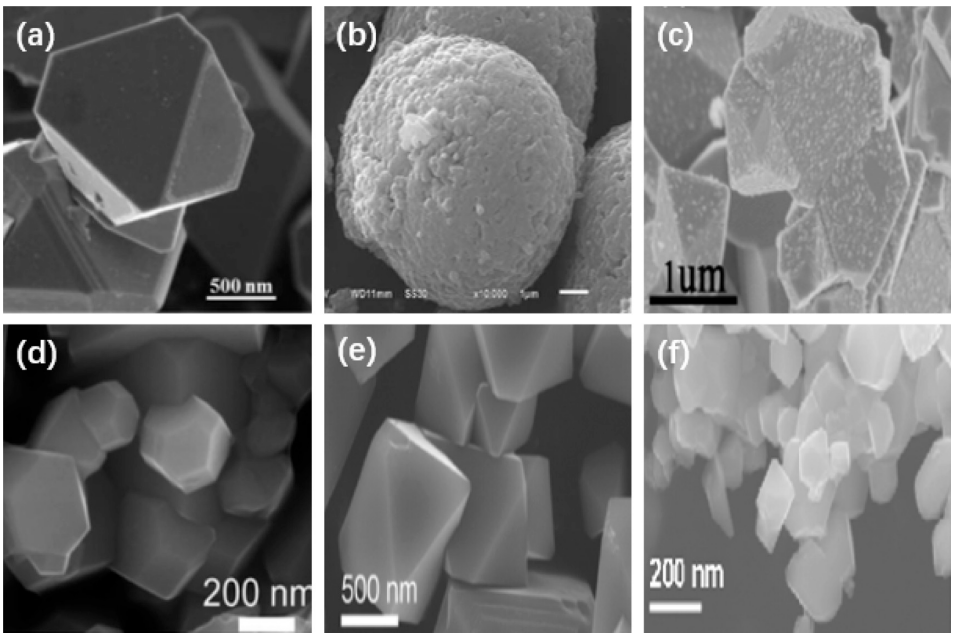

Figure 10. SEM images of (a) 2 wt % MoO_3-LMNO, reprinted with permission from ref 107. Copyright 2022 MDPI. (b) Y_2O_3-LMNO, reprinted with permission from ref 114. Copyright 2015 Springer Nature (c) 2 wt % RuO_2-LMNO, reprinted with permission from ref 115. Copyright 2015 Elsevier. (d) 3 wt % YPO_4-LMNO, reprinted with permission from ref 116. Copyright 2018 American Chemical Society. (e) 1 wt % AlF_3-LMNO, reprinted with permission from ref 118. Copyright 2015 Elsevier. (f) 5 wt % MgF_2-LMNO, reprinted with permission from ref 119. Copyright 2015 Royal Society of Chemistry.

Table 6. Characteristic of Different Coatings Using Sol−Gel Method

Synthesis method	Particle size	Lattice constant (Å)	Morphology	Surface modification	Capacity ($mAh\ g^{-1}$)/ temperature	Capacity retention (Rate/Cycle)	Remarks	ref
sol−gel	865.84 nm	8.17029	polyhedron	CNT	127.8 at 0.5C/25 °C	95.77% at 0.5C/100	-	125
	-	8.1746	spherical	F-doped Li_4SiO_4	142.5 at 0.1C/25 °C	97.8% at 4C/100	2 wt % Li_4SiO_4	126
	5 μm	8.187−8.189	polyhedron	TiO_2	113 at 1C/25 °C	99% at 1C/100	-	127
	-	-	polyhedron	La_2CO_3	126.5 at 1C/25 °C	-	1.5 wt % La_2CO_3	129
	-	-	octahedron	La_2CO_3	112.2 at 0.1C/25 °C	90.5% at 1C/100	2 wt % La_2CO_3	130
	10 nm	-	amorphous	ZrP_2O_7	120 at 1C/25 °C	80% at 1C/150	1 wt % ZrP_2O_7	109
	200−500 nm	8.1882	polyhedron	$FePO_4$	114.5 at 0.1C/25 °C	102% at 2C/80	1 wt % $FePO_4$	131
	-	-	truncated octahedron	$YBa_2Cu_3O_7$	116.7 at 2C/20 °C	87% at 2C/100 (at 60 °C)	5 wt % YBCO	132
	10 nm	-	polyhedron	$La_{0.7}Sr_{0.3}MnO_3$	124 at 2C/25 °C	90% at 2C/100	-	128
	-	-	polyhedron	$Li_4Ti_5O_{12}$	99 at 0.5C/25 °C	99% at 0.5C/100	3 wt % LTO	133
	-	-	polyhedron	$LiCoO_2$	133.6 at 0.1C/25 °C	94.35% at 2C/194	1 wt % $LiCoO_2$	134
	-	-	polyhedron	$LiNbO_3$	100 at 10C/25 °C	96.1% at 0.5C/250	1 wt % $LiNbO_3$	135
	5 μm		octahedron	$Li_{1.4}Al_{0.4}Ti_{1.6}(PO4)_3$	132.3 at 0.C/25	98.1% at 1C/100	0.5 wt % $Li_{1.4}Al_{0.4}Ti_{1.6}(PO4)_3$	136

with high electrochemical performance and crystal phases involved in the thin film that can be controlled by changing the chemical compositions of the sol.[124] Characteristics of different coatings are shown in Table 6.

Ding et al. employed carbon nanotube (CNT) coated on LMNO with a two-step calcinated process. During the synthesis process, CNT plays a crucial role: a physical barrier, size tailoring, adjusting Mn, and crystal forming assistance. This CNT coated LMNO exhibited better cycling stability and rate capability, which results in improved electrochemical performances.[125] Xu et al. designed F doped Li_4SiO_4 coated LMNO by sol−gel synthesis method. Fluorine dopant in LMNO enables increasing the bonding that can stabilize the structure and improve rate capability and cycle stability. Also, Li_4SiO_4 coating layer performs as a protective layer and superionic conductor. As a result, F doped Li_4SiO_4 coated LMNO significantly displayed better electrochemical performances.[126] LMNO coated with TiO_2 better capacity retention and smaller polarization gap due to inhibition of SEI formation. At a high temperature after cycling, TiO_2 coated LMNO maintained structural integrity.[127] Zhao et al. employed $La_{0.7}Sr_{0.3}MnO_3$ as a coating material on LMNO, which exhibited lower surface and charge/discharge resistance and higher lithium diffusion rate. It also prevents active material from HF in the electrolyte during the cycle (Figure 11).[128]

4.1.7. Solvothermal. Solvothermal synthesis is a chemical reaction that occurs in a solvent at a temperature higher than

https://doi.org/10.1021/acsomega.3c09101
ACS Omega 2024, 9, 18688−18708

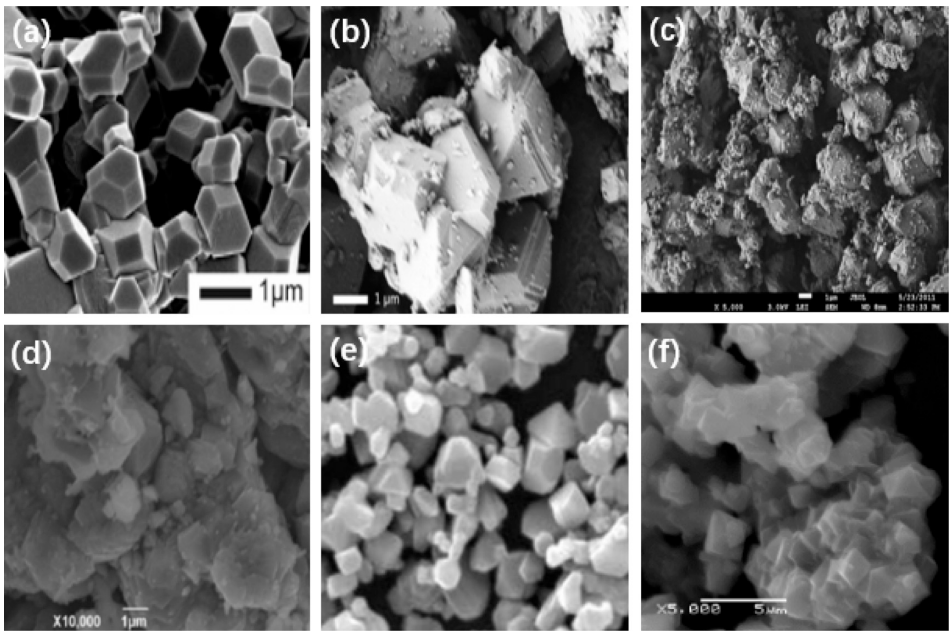

Figure 11. SEM images of (a) CNT-LMNO, reprinted with permission from ref 125. Copyright 2022 Springer Nature. (b) 5 wt % YBCO-LMNO, reprinted with permission from ref 132. Copyright 2014 Elsevier. (c) $La_{0.7}Sr_{0.3}MnO_3$-LMNO, reprinted with permission from ref 128. Copyright 2012 Elsevier. (d) 3 wt % LTO-LMNO, reprinted with permission from ref 133. Copyright 2013 Elsevier. (e) 1 wt % $LiCoO_2$-LMNO, reprinted with permission from ref 134. Copyright 2017 RSC. (f) 0.5 wt % $Li_{1.4}Al_{0.4}Ti_{1.6}(PO4)_3$-LMNO, reprinted with permission from ref 136. Copyright 2020 Elsevier.

Table 7. Characteristic of Different Coatings Using Solvothermal Method

Synthesis method	Particle size	Lattice constant (Å)	Morphology	Surface modification	Capacity (mAh g^{-1})/ temperature	Capacity retention (Rate/Cycle)	Remarks	ref
solvothermal	-	-	polyhedron	TiO_2	136 at 1C/25 °C	88.5% at 2C/500	-	143
	0.5−3 μm	8.168	octahedron	MgO	118 at C/10/25 °C	62% at C/10 to 5C/24	5 wt % MgO	139
	-	-	-	graphene	144.8 at 0.1C/25	98.5% at 0.1C/ 100	2.5 wt % GNR	140
	-	-	polyhedron	ZnO	137 at C/3/55 °C	99% at C/3/50	1.5 wt % ZnO	144
	0.5−1, 1−3 μm	8.161	-	ZnO	126 at 0.1C/25 °C	92% at 0.1C/20	1.5, 5 wt % ZnO	141
	-	8.1614	spherical	CeO_2	129.7 at 0.2C/-	98.3% at 1C/106	3 wt % CeO_2	145
	-	8.1657	polyhedron	SnO_2	145.4 at 0.2C/25 °C	75% at 2C/500	2 wt % SnO_2	146
	-	-	polyhedron	Mn_3O_4	108 at 10C/55 °C	78% at 1C/100	2.6 wt % Mn_3O_4	147
	-	-	octahedron	V_2O_5	131.5 at 1C/25 °C	92.2% at 1C/100	5 wt % V_2O_5	148
	-	8.177	spherical	Co_3O_4	120 at 10C/25 °C	95.8% at 10C/300	0.8 wt % Co	149
	7−10 μm	8.1713	spherical	CdO	133.3 at 1C/25 °C	95.2.% at 1C/300	0.4 wt % Cd	150
	-	8.16676	octahedron	Al_2O_3	129 at 1C/25 °C	92.6% at 1C/200	0.5 wt % Al_2O_3	151
	-	-	amorphous	SiO_2	130 at 0.5C/55 °C	86% at 0.5C/100	1 wt % SiO_2	152
	0.5−1 μm	8.1771	spherical	SiO_2	133.3 at 0.1C/25 °C	97.5% at 0.1C/ 100	-	153
	-	-	octahedron	RuO_2	100 at 1C/25 °C	96.1% at 0.5C/ 150	0.57 wt % RuO_2 with 1 wt % carbon additives	154
	1.5 μm	-	spherical	$Li_4Ti_5O_{12}$	112.8 at 0.5C/25 °C	93.6% at 0.5C/ 100	5 wt % LTO	142
	-	-	spherical	La_2O_3/ Al_2O_3(LAO)	124 at 1C/25 °C	94% at 1C/200	4.0 wt % (mLa_2O_3/mAl_2O_3 = 3:1)	155
	-	-	spherical	Fe_2O_3	132 at 0.5C/25 °C	98.6% at 1C/100	-	110

the boiling temperature of the solvent in a sealed vessel. Solvothermal can control over the particle shape and size through adjusting the reaction parameters. In this process, if the solvent is water, then it can be called a hydrothermal process.

This process is implemented in a sealed vessel, autoclave, offering a product which can be washed and filtered to acquire the coated sample. This coating method is used in coating morphologies: bulk powders, single and nano crystals, and thin films. In terms of process, the precursors for the coating material used by organic or nonaqueous solvent, are dissolved in solution. In addition, the cathode material that needs to be coated is added as well. The mixture is then heated at a high temperature. Types of solvent, time, temperature, concen-

https://doi.org/10.1021/acsomega.3c09101
ACS Omega 2024, 9, 18688−18708

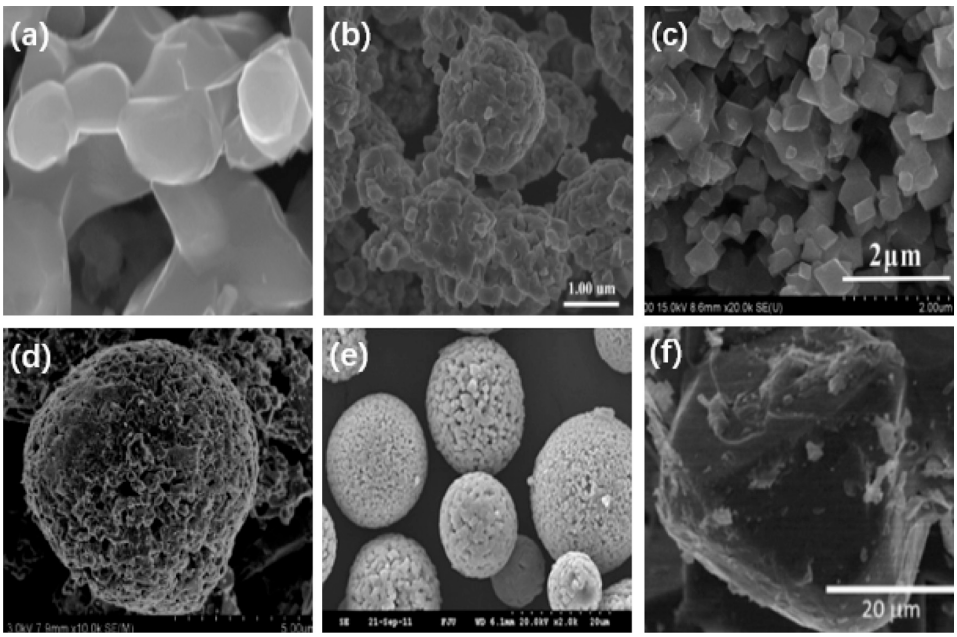

Figure 12. SEM images of (a) TiO_2-LMNO, reprinted with permission from ref 143. Copyright 2017 Elsevier. (b) CeO_2-LMNO, reprinted with permission from ref 145. Copyright 2017 Elsevier. (c) 5 wt % V_2O_5-LMNO, reprinted with permission from ref 148. Copyright 2015 Elsevier. (d) Fe_2O_3-LMNO, reprinted with permission from ref 110. Copyright 2016 Elsevier. (e) SiO_2-LMNO, reprinted with permission from ref 153. Copyright 2017 American Chemical Society. (f) 0.57 wt % RuO_2-LMNO, reprinted with permission from ref 154. Copyright 2017 Elsevier.

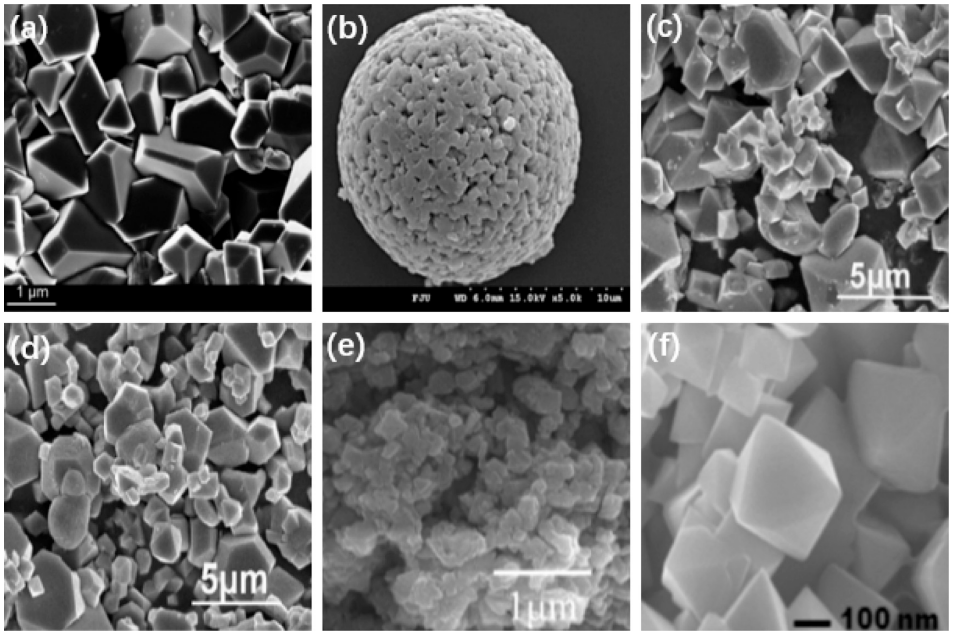

Figure 13. SEM images of (a) 0.2Fe-LMNO, reprinted with permission from ref 164. Copyright 2016 Elsevier. (b) Mg-LMNO, reprinted with permission from ref 158. Copyright 2014 Elsevier. (c) 0.06Si-LMNO, reprinted with permission from ref 166. Copyright 2020 Elsevier. (d) 0.03Ti-LMNO, reprinted with permission from ref 168. Copyright 2020 Elsevier. (e) 0.05Na-LMNO, reprinted with permission from ref 170. Copyright 2014 Elsevier. (f) 0.05Ru-LMNO, reprinted with permission from ref 173. Copyright 2015 Elsevier.

tration of precursor material and OH^- are key factors that should be considered.[28,137,138] Characteristics of different coatings are shown in Table 7.

MgO coated LMNO was presented by Alva et al. They showed MgO coated LMNO exhibited better capacity, Coulombic efficiency, and rate capability at 50 °C, especially MgO calcinated at 800 °C.[139] Xiong et al. employed sandwich structured graphene sheets (GNR) coated LMNO (GNRs@LMNO@GNRs). They mentioned GNRs enables the fast diffusion of Li ions, decreases electrochemical reaction resistance, improves the conductivity, and suppresses the volume changes, which are the factors that contribute to the electrochemical performances. The design of this LMNO exhibited higher capacity, Coulombic efficiency, and better rate capability and cycle performances.[140] Alcántara et al. showed ZnO coated LMNO using different ratio of Zn (1.5%, 5%) and preparing temperature (700 °C, 800 °C). In consequence, material prepared at 800 °C ZnO coated LMNO improves

https://doi.org/10.1021/acsomega.3c09101
ACS Omega 2024, 9, 18688−18708

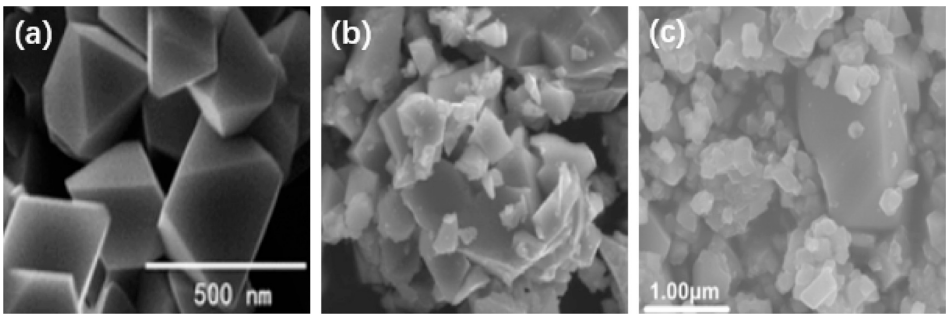

Figure 14. SEM images of (a) 0.01P-LMNO, reprinted with permission from ref 159. Copyright 2015 American Chemical Society. (b) 0.1Cl-LMNO, reprinted with permission from ref 175. Copyright 2014 Elsevier. (c) F-LMNO, reprinted with permission from ref 160. Copyright 2017 Elsevier.

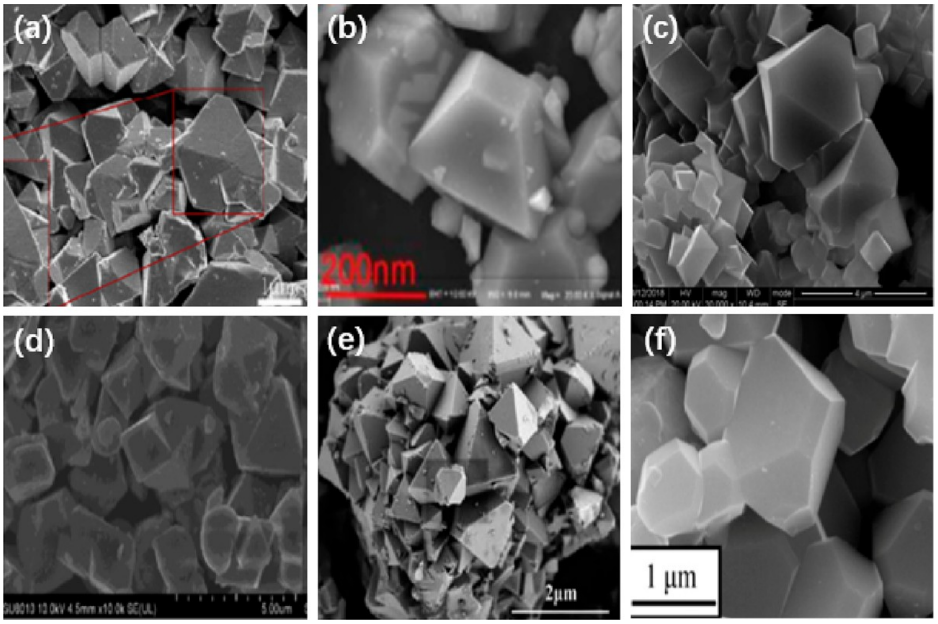

Figure 15. SEM images of (a) 0.03Cu 0.01Al-LMNO, reprinted with permission from ref 176. Copyright 2020 Elsevier. (b) 0.01Mg 0.02Y-LMNO, reprinted with permission from ref 161. Copyright 2021 Elsevier. (c) 0.03Mg 0.03Si-LMNO, reprinted with permission from ref 177. Copyright 2018 Elsevier. (d) 0.2La 1Ti-LMNO, reprinted with permission from ref 178. Copyright 2019 Elsevier. (e) 0.025Cr 0.025Ti-LMNO, reprinted with permission from ref 179. Copyright 2015 RSC. (f) 0.03Cu 0.03Al 0.03Ti-LMNO, reprinted with permission from ref 162. Copyright 2016 Elsevier.

electrochemical performances. Also, they concluded losing ZnO contributes to incorporation of Zn in the spinel structure and the formation of two cubic phases with different lattice parameters are led by electrochemical extraction of lithium.[141] Zhao et al. employed $Li_4Ti_5O_{12}$ (LTO) as a coating material on LMNO. LTO coating layers helps to suppress the reaction in electrolyte and contribute to small polarization. LTO coated LMNO exhibited high capacity retention and increased Li ion mobility, and it also showed high cyclability at high temperature (Figure 12).[142]

4.2. Effect of Doping. Like other methods to improve electrochemical performances, doping also has been found to be an effective in improving cycling and rate performances. Also, it enables to modify the properties of electrode materials such as changing the structure, composition, morphology and phase transition. It is crucial to select which doping material to use, owing to the substitution of nickel and manganese sites by dopants that promote electronic conductivity. Depending on which material to use as a dopant, LMNO can form an oxygen deficiency ($LiNi_{0.5}Mn_{1.5}O_{4-x}$) or a nickel deficiency ($Li-Ni_{0.5-x}Mn_{1.5+x}O_{4-\delta}$). In order to compensate for these oxygen and nickel deficiencies, reduction of Mn^{4+} to Mn^{3+} occurs. By replacing nickel ions to dopant ions, Mn ions can help to offset the capacity loss. In addition, Mn^{3+} ions act as internal carriers, assisting the hopping conduction mechanism and enhancing the rate of charge transfer.

Several dopants have been reported that they have been shown that it enhances the cycling stability and rate performances by using metal ion (Figure 13), nonmetal ion (Figure 14), and multi metal doping (Figure 15). As a result, the doping of ions affect the cycling stability and electrochemical performances of $LiMn_{1.5}Ni_{0.5}O_4$. Characteristics of different dopants are shown in Table 8.

Yang et al. employed Co as a dopant. Co dopant enables to completely remove NiO impurity and results in better rate capability and capacity retention.[156] A different ratio of boron was used as a dopant where 0.01 ratio of boron doped LMNO showed the best electrochemical performances. Boron doping improves Mn^{3+} ions and improves structural stability, which all contribute to enhance electrochemical performances.[157] Liu et

https://doi.org/10.1021/acsomega.3c09101
ACS Omega 2024, 9, 18688−18708

Table 8. Characteristic of Different Dopants

Property	Particle size	Lattice constant (Å)	Morphology	Dopants	Capacity (mAh g^{-1})/ temperature	Capacity retention (Rate/Cycle)	Remarks	ref
metal	3−6 μm	8.1730	octahedron	Co	130.1 at 0.1C/25 °C	92.8 at 1C/100	0.08 Co-LMNO	156
	1 μm	8.1750	octahedron	Cr	139.7 at 0.2C/25 °C	97.08% at 0.2C/40	0.15 Cr-LMNO	163
	0.737 μm	8.1760	octahedron	B	136.1 at 0.2C/25 °C	83.3% at 3C/500	0.01 B-LMNO	157
	-	8.2129	polyhedron	Fe	134 at 0.5C/25 °C	92% at 0.5C/300	0.2 Fe-LMNO	164
	-	8.1752	octahedron	Al	125 at 1C/55 °C	84% at 20C/600	0.06 Al-LMNO	165
	15 μm	8.1696	spherical	Mg	121.5 at 0.1C/25 °C	92% at 0.1C/80	-	158
	-	8.1711	octahedron	Si	135.7 at 0.2C/25 °C	91.5% at 0.2C/200	0.06 Si-LMNO	166
	3−5 μm	8.1860	polyhedron	Mo	135.6 at 0.1C/25 °C	90.5% at 0.1C/80	0.05 Mo-LMNO	167
	-	8.1880	polyhedron	Ti	127.3 at 10C/25 °C	91.7% at 1C/200	0.03 Ti-LMNO	168
	-	-	octahedron	Zr	138.4 at 1C/25 °C	95% at 1C/200	post calcined	169
	100−300 nm	8.1630	polyhedron	Na	125 at 1C/25 °C	93% at 1C/100	0.05 Na-LMNO	170
	-	8.1820	polyhedron	Cu	137.2 at 1C/25 °C	98% at 10C/100	0.05 Cu-LMNO	171
	-	8.1777	octahedron	Y	121.3 at 0.2C/25 °C	-	0.01 Y-LMNO	172
	600 nm−1 μm	8.170	octahedron	Ru	133.4 at 1C/25 °C	99.4% at 1C/150	0.05 Ru-LMNO	173
	-	8.181	octahedron	Zn	140.4 at 1C/25 °C	95% at 1C/400	0.05 Zn-LMNO	174
	-	8.167	polyhedron	Ge	133.4 at 1C/25 °C	84.9% at 1C/1000	0.02 Ge-LMNO	74
nonmetal	200−500 nm	8.1854	octahedron	P	142.7 at 0.1C/25 °C	Below 88.5% at 3C/ 300	0.01 P-LMNO	159
	5 μm	8.1913	octahedron	Cl	125.75 at 0.2C/30 °C	99% at 0.2C/40	0.1 Cl-LMNO	175
	-	8.2037	polyhedron	F	124.7 at 1C/25 °C	92.4% at 1C/300	F-LMNO	160
multimetal	-	8.1781	octahedron	Cu, Al	103.4 at 5C/25 °C	96.55 at 0.25C/100	0.03 Cu 0.01Al-LMNO	176
	-	8.1684	truncated octahedron	Mg, Y	133 at 1C/25 °C	98.49% at 1C/100	0.01 Mg 0.02Y-LMNO	161
	-	8.1803	truncated octahedron	Mg, Si	122.4 at 0.5C/25 °C	98.86 at 0.5C/100	0.03 Mg 0.03 Si-LMNO	177
	3 μm	8.1681	polyhedron	La, Ti	138.1 at 0.1C/25 °C	91% at 0.1C/300	0.5 La 1 Ti-LMNO	178
	-	8.1590	octahedron	Cr, Ti	118.7 at 10C/25 °C	102.1% at 1C/100	0.025 Cr 0.025 Ti-LMNO	179
	1 μm	8.1761	truncated octahedron	Cu, Al, Ti	137 at 0.1C/25 °C	97.9% at 0.1C/120	0.03 Cu 0.03 Al 0.03 Ti-LMNO	162

al. investigated different mole percent of Mg dopant in LMNO. Among those, Mg gradient-doped (GD) LMNO exhibited superior electrochemical performances with better discharge capacity and retention rate. It also suppresses the reaction between the electrolyte and cathode and improves Li ion diffusion.[158] Liang et al. designed Ge doped with 4s-2p orbital hybridization LMNO that exhibited long-lasting battery performance. They showed orbital hybridization of Ge 4s and O 2p orbitals contributes to strengthen the oxygen lattice.[74] Deng et al. introduced nonmetal P doped LMNO. They showed octahedral shape is maintained when less amount of P is doped. On the other hand, when excess amount of P is doped, it has truncated octahedral shape. 0.04 mol ratio of P doped LMNO showed the highest discharge capacity, and 0.01 mol ratio of P doped LMNO exhibited high retention ability. The degree of disordered transitional metal ions in LMNO is increased by the effect of P doping.[159] Nonmetal F gradient doped LMNO heated at different temperature is introduced by Luo et al. Heated at 400 °C F doped LMNO exhibited the best performance with enhanced cycling stability and high rate.[160] Co-doped LMNO with Mg and Y resulted better electrochemical performances presented by Lin et al. Mg ion helps to increase the stability of particle structure, and Y ion helps to broaden the diffusion channel of Li ions and increases the stability of lattice structure. This codoped synergistic effect made LMNO improve electrochemical performance.[161] Deng et al. employed Cu, Al, Ti tridoped LMNO. This tridoping suppresses impurity phase, enhances structural stability, and increases electronic conductivity. Ti, Al doping enhances structural stability and Al, Cu doping contributes to electronic conductivity.[162]

4.3. Cathode-Electrolyte Interface (CEI). The film formed on surface of a cathode is called cathode-electrolyte interface (CEI) which results in a loss of contact between cathode particles.[180] This CEI is formed at end of the first charge and discharge steps of the battery cell.[181] To be specific, when cathode electrochemical potential is below the energy level value of the electrolyte's highest occupied molecular orbital (HOMO), then oxidation of the conventional $LiPF_6$/organic carbonate-based electrolyte occurs. CEI can be formed through the electron transfer from the HOMO to the cathode.[44] Throughout other studies, initial CEI formation can be summarized as the following: (i) Carbonyl group of EC first absorbs on surface of the transition metal at the cathode surface. (ii) CEI formation occurs at uncovered transition metal atoms (iii) CEI formation is provoked especially at high cell potential. (iv) Transition metal coordination additives and cathode coatings can suppress the electrolyte decomposition on the cathode surface.[44,182−184] Formed CEI has a characteristic of enabling lithium-ion transfer, suppress transition metal dissolution, reduce the interfacial resistance, and inhibit structural change and side reaction between electrode and electrolyte.

Numerous researches have been conducted to figure out the CEI's chemical composition and determination through various investigation methods such as XPS[58,180,185,186] and EIS.[58,187] Duncan et al. used XPS surface measurements to study CEI in LMNO/$Li_4Ti_5O_{12}$ (LTO) cell with using conventional carbonate electrolytes ($LiPF_6$/$LiBF_4$) (Figure

https://doi.org/10.1021/acsomega.3c09101
ACS Omega 2024, 9, 18688−18708

16). They found the following: (i) All electrodes are covered with salt and organic species. (ii) Alkyl carbonates ($ROCO_2Li$)

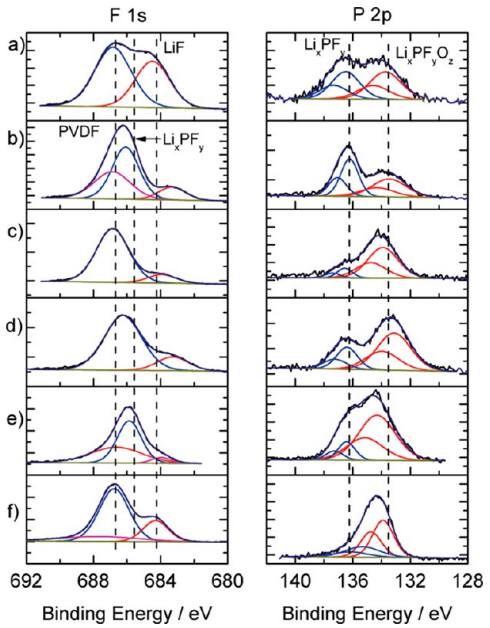

Figure 16. (Color online) F 1s and P 2p spectra of as-synthesized LMNO, EC:DEC 3:7 + 1 M $LiPF_6$ electrolyte, a) stored 24 h at 60 °C, b) stored at 0% SOC for 60 days at 60 °C, c) stored at 100% SOC for 60 days at 60 °C, d) cycled 100 times at room temperature, e) cycled 100 times at 60 °C f) cycled 100 times at room temperature, LTO negative electrode, reprinted with permission from ref 187. Copyright 2011 Electrochemical Society.

and polyethers compose the organic layer. Also, Li_2CO_3 was detected in the electrode that was stored at 60 °C without cycling, whereas polycarbonate, represented as $-[OCO2-]_x-$, was found on the electrode that was stored or cycled at 60 °C. (iii) Depending on which electrolyte to use, $Li_xPF_yO_z$ or $Li_xBF_yO_z$ composes the salt layer, along with LiF that is present on all cells.[187] In another study, Yoon et al. used Al_2O_3 coating as a HF scavenger that made CEI relatively stable. In this study, EIS spectra showed that resistance of the CEI on the LMNO, coated with Al_2O_3, was relatively stable, but uncoated LMNO displayed sharp decrease (Figure 17).[58]

5. CONCLUSION AND PERSPECTIVES

This Review summarizes the four major aspects of $LiMn_{1.5}Ni_{0.5}O_4$ (LMNO) cathode material which all influence the characteristics and electrical performances: (i) coating strategy (ii) doping strategy, (iv) electrolyte, and (v) oxygen deficiency. As discussed earlier, LMNO has various spinel phases that have different characteristics, which depend on different temperature or oxygen deficiency, and it transforms from ordered phase, $P4_332$, to disordered phase, to rock salt phase. Furthermore, during cycling, intercalation/extraction of lithium ions can be detected and leads to unwanted side reaction at the LMNO/electrolyte interface. Therefore, different methods have been proposed to suppress the unwanted side reaction through both surface modification and doping. By using various synthesis method (i.e., chemical vapor deposition process (CVD), dry coating, atomic layer deposition (ALD), coprecipitation, radio frequency magnetron sputtering, sol−gel, solvothermal) with different materials, using different dopants, adding additive in electrolyte, and controlling oxygen radicals, it all made LMNO possible to enhance the electrochemical performances. Likewise, these factors have been proven to play a crucial role in LMNO. For the further development, herein we propose our perspectives:

(1) Through surface modification, doping, surface control in the half-cell configuration, electrochemical performance improvements are shown. However, when it comes to full-cell configuration with graphite anode, capacity fade still remains as a problem. To be specific, gradual consumption of Li ions in SEI layer on the graphite anode affects capacity fade. Therefore, a different approach is needed to design the cell, and which materials should be used as an anode should be considered.

(2) Through many studies, it has proven that LMNO becomes stable with variety of methods in the room temperature. However, when the half cell is tested at low or high temperature, it becomes very unstable. As a result, studying different characteristics of the element is necessary.

(3) According to the experimental results done in electrolytes, electrolyte decomposition is one of the problems that has to be considered. Especially, since LMNO operates at high voltage (5 V), it is necessary to find the proper electrolyte that corresponds with the LMNO. For instance, studying alternative liquid electrolytes that have less reaction with metal ion dissolution or solid electrolytes with high lithium ion conductivity and compatible interface is needed.

(4) For the stability of LMNO, understanding the phase transition is necessary. Through different formation of LMNO, it has different characteristics. By understanding

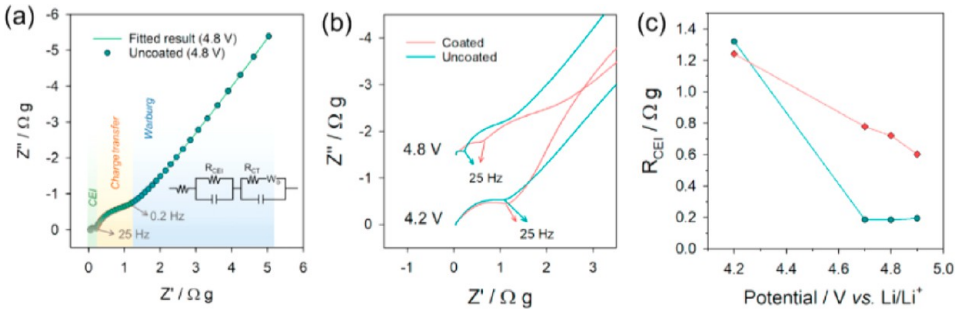

Figure 17. (a) A representative EIS data and the fitting curve. (b) EIS spectra obtained at 4.2 and 4.8 V for both the Al_2O_3 coated and uncoated LNMO electrodes. (c) Variations in CEI resistance with increasing potential, reprinted with permission from ref 58. Copyright 2021 Elsevier.

https://doi.org/10.1021/acsomega.3c09101
ACS Omega 2024, 9, 18688−18708

these factors, it is possible to control the LMNO phases. For example, since LMNO is sensitive to temperature, deciding on which temperature to sinter can affect the stability. Another factor is proton intercalation which affects the stability. During the decomposition reaction, intercalation of Li ion decreases and triggers proton intercalation and surface reconstruction in spinel structure. Therefore, a proton free mechanism should be considered.

In conclusion, among the many strategies that led to better electrochemical performances for LMNO, we believe that the doping strategy is more likely to be commercialized. Besides using either metal/nonmetal or multimetal ions as mentioned in section 4.2, high entropy cathodes are emerging as a new class of material. High entropy, using multiple element (at least five) to make a single phase system, is used in various fields, such as catalysis, energy storage, and others.[188] Owing to its outstanding properties, such as structure stability and strength, in recent years, this strategy has been extended to oxide cathode materials.[189,190] Even though there are few reported studies about high entropy cathode materials, we believe there is no doubt that this strategy will not only contribute to optimized electrochemical performances but also makes feasible the commercialization of batteries in the next generation.

AUTHOR INFORMATION

Corresponding Author

Yongyao Xia − *Department of Chemistry and Shanghai Key Laboratory of Molecular Catalysis and Innovative Materials, Institute of New Energy, iChEM (Collaborative Innovation Center of Chemistry for Energy Materials), Fudan University, Shanghai 200433, China;* orcid.org/0000-0001-6379-9655; Email: yyxia@fudan.edu.cn

Authors

Seokyoung Choi − *Department of Chemistry and Shanghai Key Laboratory of Molecular Catalysis and Innovative Materials, Institute of New Energy, iChEM (Collaborative Innovation Center of Chemistry for Energy Materials), Fudan University, Shanghai 200433, China*

Wuliang Feng − *Institute for Sustainable Energy & College of Sciences, Shanghai University, Shanghai 200444, China*

Complete contact information is available at: https://pubs.acs.org/10.1021/acsomega.3c09101

Notes

The authors declare no competing financial interest.

ACKNOWLEDGMENTS

This work was supported by the National Key Research and Development Program of China (2023YFB2405800).

REFERENCES

(1) Schlögl, R. Chemical energy storage enables the transformation of fossil energy systems to sustainability. *Green Chem.* **2021**, *23* (4), 1584−1593.

(2) Chen, M.; Zhang, Y.; Xing, G.; Chou, S.-L.; Tang, Y. Electrochemical energy storage devices working in extreme conditions. *Energy Environ. Sci.* **2021**, *14* (6), 3323−3351.

(3) Shen, K.; Xu, X.; Tang, Y. Recent progress of magnetic field application in lithium-based batteries. *Nano Energy* **2022**, *92*, 106703.

(4) George, G.; George, K.; Aitor, E.-B.; Miguel, B.; Iratxe de, M.; Georgia, K. Aerosol Spray Pyrolysis Synthesis of Doped LiNi0.5Mn1.5O4 Cathode Materials for Next Generation Lithium-Ion Batteries. In *Recent Perspectives in Pyrolysis Research*; Mattia, B., Mauro, G., Eds.; IntechOpen, 2022; p Ch. 10.

(5) Palaniyandy, N.; Reddy, M. V.; Zaghib, K.; Kebede, M. A.; Raju, K.; Modibedi, R. M.; Mathe, M. K.; Abhilash, K. P.; Balamuralikrishnan, S. High rate and stable capacity performance of 2D LiMn1.5Ni0.5O4 nanoplates cathode with ultra-long cycle stability. *J. Alloys Compd.* **2022**, *903*, 163869.

(6) Bi, X.; Chang, L.; Cao, S.; Luo, S.; Yang, W.; Wei, A.; Yang, R.; Liu, J. Preparation and Improvement of Electrochemical Performance of LiNi0.5Mn1.5O4 Cathode Materials In Situ Coated with AlPO4. *Energy Fuels* **2023**, *37* (4), 3236−3246.

(7) Huang, Z.-X.; Zhang, X.-L.; Zhao, X.-X.; Heng, Y.-L.; Wang, T.; Geng, H.; Wu, X.-L. Hollow Na0.62K0.05Mn0.7Ni0.2Co0.1O2 polyhedra with exposed stable {001} facets and K riveting for sodium-ion batteries. *Science China Materials* **2023**, *66* (1), 79−87.

(8) Huang, Z.-X.; Zhang, X.-L.; Zhao, X.-X.; Lü, H.-Y.; Zhang, X.-Y.; Heng, Y.-L.; Geng, H.; Wu, X.-L. Suppressing oxygen redox in layered oxide cathode of sodium-ion batteries with ribbon superstructure and solid-solution behavior. *Journal of Materials Science & Technology* **2023**, *160*, 9−17.

(9) Dahn, J. R.; Fuller, E. W.; Obrovac, M.; von Sacken, U. Thermal stability of LixCoO2, LixNiO2 and λ-MnO2 and consequences for the safety of Li-ion cells. *Solid State Ionics* **1994**, *69* (3), 265−270.

(10) Kim, T.-H.; Park, J.-S.; Chang, S. K.; Choi, S.; Ryu, J. H.; Song, H.-K. The Current Move of Lithium Ion Batteries Towards the Next Phase. *Adv. Energy Mater.* **2012**, *2* (7), 860−872.

(11) Nitta, N.; Wu, F.; Lee, J. T.; Yushin, G. Li-ion battery materials: present and future. *Mater. Today* **2015**, *18* (5), 252−264.

(12) Väyrynen, A.; Salminen, J. Lithium ion battery production. *J. Chem. Thermodyn.* **2012**, *46*, 80−85.

(13) Pieczonka, N. P. W.; Liu, Z.; Huq, A.; Kim, J.-H. Comparative study of LiMnPO4/C cathodes synthesized by polyol and solid-state reaction methods for Li-ion batteries. *J. Power Sources* **2013**, *230*, 122−129.

(14) Liu, G.; Zhang, J.; Zhang, X.; Du, Y.; Zhang, K.; Li, G.; Yu, H.; Li, C.; Li, Z.; Sun, Q.; Wen, L. Study on oxygen deficiency in spinel LiNi0.5Mn1.5O4 and its Fe and Cr-doped compounds. *J. Alloys Compd.* **2017**, *725*, 580−586.

(15) Sahoo, K.; Majhi, J.; Mitra, A.; Kumar, A. S.; Majumder, S. Investigations on the electrochemical characteristics of rechargeable MCMB-LiNi0. 5Mn1. 5O4 pouch cells. *J. Electrochem. Soc.* **2019**, *166* (2), A342.

(16) Zou, B.; Hu, Q.; Qu, D.; Yu, R.; Zhou, Y.; Tang, Z.; Chen, C. A high energy density full lithium-ion cell based on specially matched coulombic efficiency. *Journal of Materials Chemistry A* **2016**, *4* (11), 4117−4124.

(17) Bi, K.; Zhao, S.-X.; Huang, C.; Nan, C.-W. Improving low-temperature performance of spinel LiNi0.5Mn1.5O4 electrode and LiNi0.5Mn1.5O4/Li4Ti5O12 full-cell by coating solid-state electrolyte Li-Al-Ti-P-O. *J. Power Sources* **2018**, *389*, 240−248.

(18) Aktekin, B.; Valvo, M.; Smith, R. I.; Sørby, M. H.; Lodi Marzano, F.; Zipprich, W.; Brandell, D.; Edström, K.; Brant, W. R. Cation Ordering and Oxygen Release in LiNi0.5-xMn1.5+xO4-y (LNMO): In Situ Neutron Diffraction and Performance in Li Ion Full Cells. *ACS Applied Energy Materials* **2019**, *2* (5), 3323−3335.

(19) Wang, F.; Borodin, O.; Ding, M. S.; Gobet, M.; Vatamanu, J.; Fan, X.; Gao, T.; Eidson, N.; Liang, Y.; Sun, W.; et al. Hybrid aqueous/non-aqueous electrolyte for safe and high-energy Li-ion batteries. *Joule* **2018**, *2* (5), 927−937.

(20) Michalak, B.; Sommer, H.; Mannes, D.; Kaestner, A.; Brezesinski, T.; Janek, J. Gas evolution in operating lithium-ion batteries studied in situ by neutron imaging. *Sci. Rep.* **2015**, *5* (1), 15627.

(21) Arun, N.; Aravindan, V.; Jayaraman, S.; Madhavi, S. Unveiling the fabrication of "rocking-chair" type 3.2 and 1.2 V class cells using

spinel LiNi0. 5Mn1. 5O4 as cathode with Li4Ti5O12. *J. Phys. Chem. C* **2015**, *119* (43), 24332−24336.
(22) Cen, J.; Zhu, B.; Kavanagh, S. R.; Squires, A. G.; Scanlon, D. O. Cation disorder dominates the defect chemistry of high-voltage LiMn 1.5 Ni 0.5 O 4 (LMNO) spinel cathodes. *Journal of Materials Chemistry A* **2023**, *11*, 13353.
(23) Cen, J.; Zhu, B.; Kavanagh, S.; Squires, A.; Scanlon, D. Intrinsic Defect Chemistry of High-Voltage LiMn1.5Ni0.5O4 (LMNO) Spinel Cathode. *ChemRxiv*, Jan. 27, **2023**, ver. 2.
(24) Shiiba, H.; Zettsu, N.; Nakayama, M.; Oishi, S.; Teshima, K. Defect formation energy in spinel LiNi0. 5Mn1. 5O4-δ using Ab initio DFT calculations. *J. Phys. Chem. C* **2015**, *119* (17), 9117−9124.
(25) Bhatia, A.; Cretu, S.; Hallot, M.; Folastre, N.; Berthe, M.; Troadec, D.; Roussel, P.; Pereira-Ramos, J.-P.; Baddour-Hadjean, R.; Lethien, C.; Demortière, A. In Situ Liquid Electrochemical TEM Investigation of LiMn1.5Ni0.5O4 Thin Film Cathode for Micro-Battery Applications. *Small Methods* **2022**, *6* (2), 2100891.
(26) Gabrielli, G.; Axmann, P.; Diemant, T.; Behm, R. J.; Wohlfahrt-Mehrens, M. Combining Optimized Particle Morphology with a Niobium-Based Coating for Long Cycling-Life, High-Voltage Lithium-Ion Batteries. *ChemSusChem* **2016**, *9* (13), 1670−1679.
(27) Radzi, Z.I.; Balakrishnan, V.; Pandey, A.K.; Kufian, M.Z.; Rahim, N.A.; Raihan, S.R.S.; Ramesh, S. Structural, electrical and electrochemical characterization of hybrid morphological LiNi0.5Mn1.5O4 cathode material. *Physica B: Condensed Matter* **2022**, *624*, 413376.
(28) Qureshi, Z. A.; Tariq, H. A.; Shakoor, R. A.; Kahraman, R.; AlQaradawi, S. Impact of coatings on the electrochemical performance of LiNi0.5Mn1.5O4 cathode materials: A focused review. *Ceram. Int.* **2022**, *48* (6), 7374−7392.
(29) Amin, R.; Muralidharan, N.; Petla, R. K.; Ben Yahia, H.; Jassim Al-Hail, S. A.; Essehli, R.; Daniel, C.; Khaleel, M. A.; Belharouak, I. Research advances on cobalt-free cathodes for Li-ion batteries - The high voltage LiMn1.5Ni0.5O4 as an example. *J. Power Sources* **2020**, *467*, 228318.
(30) Yi, T.-F.; Xie, Y.; Zhu, Y.-R.; Zhu, R.-S.; Ye, M.-F. High rate micron-sized niobium-doped LiMn1.5Ni0.5O4 as ultra high power positive-electrode material for lithium-ion batteries. *J. Power Sources* **2012**, *211*, 59−65.
(31) Tan, C.; Yang, J.; Pan, Q.; Li, Y.; Li, Y.; Cui, L.; Fan, X.; Zheng, F.; Wang, H.; Li, Q. Optimizing interphase structure to enhance electrochemical performance of high voltage LiNi0.5Mn1.5O4 cathode via anhydride additives. *Chemical Engineering Journal* **2021**, *410*, 128422.
(32) Luo, X. Improvement of the electrochemical performance of spinel LiNi0.5Mn1.5O4 by stabilization of the electrode/electrolyte interfaces with the electrolyte additive. *J. Alloys Compd.* **2018**, *730*, 23−30.
(33) Zhang, H.; Liu, H.; Piper, L. F. J.; Whittingham, M. S.; Zhou, G. Oxygen Loss in Layered Oxide Cathodes for Li-Ion Batteries: Mechanisms, Effects, and Mitigation. *Chem. Rev.* **2022**, *122* (6), 5641−5681.
(34) Kim, J. H.; Myung, S. T.; Yoon, C. S.; Kang, S. G.; Sun, Y. K. Comparative Study of LiNi0.5Mn1.5O4-δ and LiNi0.5Mn1.5O4 Cathodes Having Two Crystallographic Structures: Fd$\bar{3}$m and P4332. *Chem. Mater.* **2004**, *16* (5), 906−914.
(35) Lee, J.; Kim, C.; Kang, B. High electrochemical performance of high-voltage LiNi0.5Mn1.5O4 by decoupling the Ni/Mn disordering from the presence of Mn3+ ions. *NPG Asia Materials* **2015**, *7* (8), No. e211.
(36) Wang, F.; Suo, L.; Liang, Y.; Yang, C.; Han, F.; Gao, T.; Sun, W.; Wang, C. Spinel LiNi0.5Mn1.5O4 Cathode for High-Energy Aqueous Lithium-Ion Batteries. *Adv. Energy Mater.* **2017**, *7* (8), 1600922.
(37) Martens, I.; Vostrov, N.; Mirolo, M.; Colalongo, M.; Kúš, P.; Richard, M.-I.; Wang, L.; Zhu, X.; Schülli, T. U.; Drnec, J. Revisiting Phase Transformation Mechanisms in LiNi0.5Mn1.5O4 High Voltage Cathodes with Operando Microdiffraction. *ACS Materials Letters* **2022**, *4* (12), 2528−2536.
(38) Zheng, J.; Xiao, J.; Yu, X.; Kovarik, L.; Gu, M.; Omenya, F.; Chen, X.; Yang, X.-Q.; Liu, J.; Graff, G. L.; et al. Enhanced Li+ ion transport in LiNi0.5Mn1.5O4 through control of site disorder. *Phys. Chem. Chem. Phys.* **2012**, *14* (39), 13515−13521.
(39) Jafta, C. J.; Mathe, M. K.; Manyala, N.; Roos, W. D.; Ozoemena, K. I. Microwave-Assisted Synthesis of High-Voltage Nanostructured LiMn1.5Ni0.5O4 Spinel: Tuning the Mn3+ Content and Electrochemical Performance. *ACS Appl. Mater. Interfaces* **2013**, *5* (15), 7592−7598.
(40) Kim, J. H.; Yoon, C. S.; Myung, S. T.; Prakash, J.; Sun, Y. K. Phase Transitions in Li1 - δ Ni0.5Mn1.5 O 4 during Cycling at 5 V. *Electrochem. Solid-State Lett.* **2004**, *7* (7), A216.
(41) Manthiram, A.; Chemelewski, K.; Lee, E.-S. A perspective on the high-voltage LiMn1.5Ni0.5O4 spinel cathode for lithium-ion batteries. *Energy Environ. Sci.* **2014**, *7* (4), 1339−1350.
(42) Kim, J.; Hong, Y.; Ryu, K. S.; Kim, M. G.; Cho, J. Washing Effect of a LiNi0.83Co0.15Al0.02O2 Cathode in Water. *Electrochem. Solid-State Lett.* **2006**, *9* (1), A19.
(43) Zhuang, G. V.; Chen, G.; Shim, J.; Song, X.; Ross, P. N.; Richardson, T. J. Li2CO3 in LiNi0.8Co0.15Al0.05O2 cathodes and its effects on capacity and power. *J. Power Sources* **2004**, *134* (2), 293−297.
(44) Kühn, S. P.; Edström, K.; Winter, M.; Cekic-Laskovic, I. Face to Face at the Cathode Electrolyte Interphase: From Interface Features to Interphase Formation and Dynamics. *Advanced Materials Interfaces* **2022**, *9* (8), 2102078.
(45) Freiberg, A. T. S.; Sicklinger, J.; Solchenbach, S.; Gasteiger, H. A. Li2CO3 decomposition in Li-ion batteries induced by the electrochemical oxidation of the electrolyte and of electrolyte impurities. *Electrochim. Acta* **2020**, *346*, 136271.
(46) Hong, J.; Lim, H.-D.; Lee, M.; Kim, S.-W.; Kim, H.; Oh, S.-T.; Chung, G.-C.; Kang, K. Critical Role of Oxygen Evolved from Layered Li-Excess Metal Oxides in Lithium Rechargeable Batteries. *Chem. Mater.* **2012**, *24* (14), 2692−2697.
(47) von Cresce, A.; Xu, K. Electrolyte Additive in Support of 5V Li Ion Chemistry. *J. Electrochem. Soc.* **2011**, *158*, A337.
(48) Robinson, J. P.; Kichambare, P. D.; Deiner, J. L.; Miller, R.; Rottmayer, M. A.; Koenig, G. M., Jr High temperature electrode-electrolyte interface formation between LiMn1.5Ni0.5O4 and Li1.4Al0.4Ge1.6(PO4)3. *J. Am. Ceram. Soc.* **2018**, *101* (3), 1087−1094.
(49) Zheng, X.; Liao, Y.; Zhang, Z.; Zhu, J.; Ren, F.; He, H.; Xiang, Y.; Zheng, Y.; Yang, Y. Exploring high-voltage fluorinated carbonate electrolytes for LiNi0.5Mn1.5O4 cathode in Li-ion batteries. *Journal of Energy Chemistry* **2020**, *42*, 62−70.
(50) Lee, T. J.; Lee, J. B.; Yoon, T.; Kim, D.; Chae, O. B.; Jung, J.; Soon, J.; Ryu, J. H.; Kim, J. J.; Oh, S. M. Tris(pentafluorophenyl)-silane as an Electrolyte Additive for 5 V LiNi0.5Mn1.5O4 Positive Electrode. *J. Electrochem. Soc.* **2016**, *163* (6), A898.
(51) Xu, M.; Lu, D.; Garsuch, A.; Lucht, B. L. Improved Performance of LiNi0.5Mn1.5O4 Cathodes with Electrolytes Containing Dimethylmethylphosphonate (DMMP). *J. Electrochem. Soc.* **2012**, *159* (12), A2130.
(52) Perea, A.; Zaghib, K.; Bélanger, D. Characterization of LiNi0.5Mn1.5O4 spinel electrode in the presence of 1,3,5-trihydroxybenzene as additive. *Journal of Materials Chemistry A* **2015**, *3* (6), 2776−2783.
(53) Ma, Y.; Ma, J.; Chai, J.; Liu, Z.; Ding, G.; Xu, G.; Liu, H.; Chen, B.; Zhou, X.; Cui, G.; Chen, L. Two Players Make a Formidable Combination: In Situ Generated Poly(acrylic anhydride-2-methyl-acrylic acid-2-oxirane-ethyl ester-methyl methacrylate) Cross-Linking Gel Polymer Electrolyte toward 5 V High-Voltage Batteries. *ACS Appl. Mater. Interfaces* **2017**, *9* (47), 41462−41472.
(54) Xu, M.; Zhou, L.; Dong, Y.; Chen, Y.; Demeaux, J.; MacIntosh, A. D.; Garsuch, A.; Lucht, B. L. Development of novel lithium borate additives for designed surface modification of high voltage LiNi0.5Mn1.5O4 cathodes. *Energy Environ. Sci.* **2016**, *9* (4), 1308−1319.

https://doi.org/10.1021/acsomega.3c09101
ACS Omega 2024, 9, 18688−18708

(55) Li, S. R.; Sinha, N. N.; Chen, C. H.; Xu, K.; Dahn, J. R. A Consideration of Electrolyte Additives for LiNi0.5Mn1.5O4/Li4Ti5O12 Li-Ion Cells. *J. Electrochem. Soc.* **2013**, *160* (11), A2014.
(56) Fu, C.; Homann, G.; Grissa, R.; Rentsch, D.; Zhao, W.; Gouveia, T.; Falgayrat, A.; Lin, R.; Fantini, S.; Battaglia, C. A Polymerized-Ionic-Liquid-Based Polymer Electrolyte with High Oxidative Stability for 4 and 5 V Class Solid-State Lithium Metal Batteries. *Adv. Energy Mater.* **2022**, *12* (27), 2200412.
(57) Zhang, L.; Guo, H.; Zhang, Q.; Wang, A.; Su, Y.; Chen, Y.; Li, Y.; Shen, F.; Han, X. In Situ Formed Surface Layer to Improve the Air Stability of LLZTO and Its Contact with the Li Metal. *Energy Fuels* **2023**, *37* (18), 14341−14349.
(58) Yoon, T.; Soon, J.; Lee, T. J.; Ryu, J. H.; Oh, S. M. Dissolution of cathode-electrolyte interphase deposited on LiNi0.5Mn1.5O4 for lithium-ion batteries. *J. Power Sources* **2021**, *503*, 230051.
(59) Xu, M.; Zhou, L.; Dong, Y.; Chen, Y.; Garsuch, A.; Lucht, B. L. Improving the Performance of Graphite/ LiNi0.5Mn1.5O4 Cells at High Voltage and Elevated Temperature with Added Lithium Bis(oxalato) Borate (LiBOB). *J. Electrochem. Soc.* **2013**, *160* (11), A2005.
(60) Zhang, L.; Ma, Y.; Cheng, X.; Zuo, P.; Cui, Y.; Guan, T.; Du, C.; Gao, Y.; Yin, G. Enhancement of high voltage cycling performance and thermal stability of LiNi1/3Co1/3Mn1/3O2 cathode by use of boron-based additives. *Solid State Ionics* **2014**, *263*, 146−151.
(61) Dong, Y.; Demeaux, J.; Zhang, Y.; Lucht, B. L. Improving the Performance of Graphite/LiNi0.5Mn1.5O4 Cells with Added N,N-dimethylformamide Sulfur Trioxide Complex. *J. Electrochem. Soc.* **2017**, *164* (13), A3182.
(62) Hu, L.; Zhang, Z.; Amine, K. Fluorinated electrolytes for Li-ion battery: An FEC-based electrolyte for high voltage LiNi0.5Mn1.5O4/graphite couple. *Electrochem. Commun.* **2013**, *35*, 76−79.
(63) Song, Y.-M.; Han, J.-G.; Park, S.; Lee, K. T.; Choi, N.-S. A multifunctional phosphite-containing electrolyte for 5 V-class LiNi0.5Mn1.5O4 cathodes with superior electrochemical performance. *Journal of Materials Chemistry A* **2014**, *2* (25), 9506−9513.
(64) Dong, Y.; Demeaux, J.; Zhang, Y.; Xu, M.; Zhou, L.; MacIntosh, A. D.; Lucht, B. L. Improving the Performance at Elevated Temperature of High Voltage Graphite/LiNi0.5Mn1.5O4 Cells with Added Lithium Catechol Dimethyl Borate. *J. Electrochem. Soc.* **2017**, *164* (2), A128.
(65) Wang, L.; Li, H.; Huang, X.; Baudrin, E. A comparative study of Fd-3m and P4332 "LiNi0.5Mn1.5O4. *Solid State Ionics* **2011**, *193* (1), 32−38.
(66) Pasero, D.; Reeves, N.; Pralong, V.; West, A. R. Oxygen Nonstoichiometry and Phase Transitions in LiMn1.5Ni0.5O4 - δ. *J. Electrochem. Soc.* **2008**, *155* (4), A282.
(67) Kunduraci, M.; Amatucci, G. G. Synthesis and Characterization of Nanostructured 4.7 V Lix Mn1.5Ni0.5O4 Spinels for High-Power Lithium-Ion Batteries. *J. Electrochem. Soc.* **2006**, *153* (7), A1345.
(68) Kasnatscheew, J.; Evertz, M.; Streipert, B.; Wagner, R.; Nowak, S.; Cekic Laskovic, I.; Winter, M. Improving cycle life of layered lithium transition metal oxide (LiMO2) based positive electrodes for Li ion batteries by smart selection of the electrochemical charge conditions. *J. Power Sources* **2017**, *359*, 458−467.
(69) Yu, X.; Lyu, Y.; Gu, L.; Wu, H.; Bak, S.-M.; Zhou, Y.; Amine, K.; Ehrlich, S. N.; Li, H.; Nam, K.-W.; Yang, X.-Q. Understanding the Rate Capability of High-Energy-Density Li-Rich Layered Li1.2Ni0.15-Co0.1Mn0.55O2 Cathode Materials. *Adv. Energy Mater.* **2014**, *4* (5), 1300950.
(70) Broussely, M.; Biensan, P.; Bonhomme, F.; Blanchard, P.; Herreyre, S.; Nechev, K.; Staniewicz, R. J. Main aging mechanisms in Li ion batteries. *J. Power Sources* **2005**, *146* (1), 90−96.
(71) Wang, Y.; Yi, J.; Xia, Y. Recent Progress in Aqueous Lithium-Ion Batteries. *Adv. Energy Mater.* **2012**, *2* (7), 830−840.
(72) Sudaryanto; Fakhrudin, M.; Purwamargapratala, Y.; Yulianti, E.; Deswita; Wahyudianingsih. Synthesis of rare Earth element doped LiMn1.5Ni0.5O4 as a lithium-ion battery cathode material using sonochemical method. *AIP Conf. Proc.* **2021**, *2381*, 020084.
(73) Chen, Z.; Qin, Y.; Amine, K.; Sun, Y. K. Role of surface coating on cathode materials for lithium-ion batteries. *J. Mater. Chem.* **2010**, *20* (36), 7606−7612.
(74) Liang, G.; Olsson, E.; Zou, J.; Wu, Z.; Li, J.; Lu, C.-Z.; D'Angelo, A. M.; Johannessen, B.; Thomsen, L.; Cowie, B.; et al. Introducing 4s-2p Orbital Hybridization to Stabilize Spinel Oxide Cathodes for Lithium-Ion Batteries. *Angew. Chem., Int. Ed.* **2022**, *61* (27), No. e202201969.
(75) Ravikumar, B.; Mynam, M.; Rai, B. Effect of Salt Concentration on Properties of Lithium Ion Battery Electrolytes: A Molecular Dynamics Study. *J. Phys. Chem. C* **2018**, *122* (15), 8173−8181.
(76) Tong, Z.; Ye, Q.; Deng, Y.; She, Q.; Huang, A.; Xu, J.; Zhu, X. Tuning the structural disordering in hierarchical LiNi0.5Mn1.5O4 microrods for stable high-rate electrode performance. *J. Alloys Compd.* **2023**, *937*, 168544.
(77) Sun, Y.; Yang, Y.; Zhan, H.; Shao, H.; Zhou, Y. Synthesis of high power type LiMn1.5Ni0.5O4 by optimizing its preparation conditions. *J. Power Sources* **2010**, *195* (13), 4322−4326.
(78) Kebede, M. A. An investigation of the lattice parameter and micro-strain behaviour of LiMn2O4 coated with LiMn1.5Ni0.5O4 to attain high-rate capability and cycling stability. *Journal of Energy Storage* **2023**, *72*, 108602.
(79) Karunawan, J.; Suryadi, P. N.; Mahfudh, L.; Santosa, S. P.; Sumboja, A.; Iskandar, F. Truncated Octahedral Shape of Spinel LiNi0.5Mn1.5O4 via a Solid-State Method for Li-Ion Batteries. *Energy Fuels* **2023**, *37* (1), 754−762.
(80) Sun, L.; Yuan, G.; Gao, L.; Yang, J.; Chhowalla, M.; Gharahcheshmeh, M. H.; Gleason, K. K.; Choi, Y. S.; Hong, B. H.; Liu, Z. Chemical vapour deposition. *Nature Reviews Methods Primers* **2021**, *1* (1), 5.
(81) Lee, Y.; Kim, T. Y.; Kim, D.-W.; Lee, J. K.; Choi, W. Coating of spinel LiNi0.5Mn1.5O4 cathodes with SnO2 by an electron cyclotron resonance metal-organic chemical vapor deposition method for high-voltage applications in lithium ion batteries. *J. Electroanal. Chem.* **2015**, *736*, 16−21.
(82) Sun, P.; Ma, Y.; Zhai, T.; Li, H. High performance LiNi0.5Mn1.5O4 cathode by Al-coating and Al3+-doping through a physical vapor deposition method. *Electrochim. Acta* **2016**, *191*, 237−246.
(83) Nakamura, H.; Kawaguchi, T.; Masuyama, T.; Sakuda, A.; Saito, T.; Kuratani, K.; Ohsaki, S.; Watano, S. Dry coating of active material particles with sulfide solid electrolytes for an all-solid-state lithium battery. *J. Power Sources* **2020**, *448*, 227579.
(84) Pfeffer, R.; Dave, R. N.; Wei, D.; Ramlakhan, M. Synthesis of engineered particulates with tailored properties using dry particle coating. *Powder Technol.* **2001**, *117* (1), 40−67.
(85) Kawaguchi, T.; Nakamura, H.; Watano, S. Dry coating of electrode particle with model particle of sulfide solid electrolytes for all-solid-state secondary battery. *Powder Technol.* **2018**, *323*, 581−587.
(86) Yang, J.; Slíva, A.; Banerjee, A.; Dave, R.; Pfeffer, R. Dry Particle Coating for Improving the Flowability of Cohesive Powders. *Powder Technology* **2005**, *158*, 21.
(87) Nisar, U.; Al-Hail, S. A. J. A.; Petla, R. K.; Shakoor, R. A.; Essehli, R.; Kahraman, R.; AlQaradawi, S. Y.; Kim, D. K.; Belharouak, I.; Amin, M. R. Understanding the Origin of the Ultrahigh Rate Performance of a SiO2-Modified LiNi0.5Mn1.5O4 Cathode for Lithium-Ion Batteries. *ACS Applied Energy Materials* **2019**, *2* (10), 7263−7271.
(88) Cho, S.; Kim, S.; Kim, W.; Kim, S. Study on Electrochemical Performance of Various Oxides-Coated LiNi0.5Mn1.5O4 Cathode for Lithium Ion Battery. *Electronic Materials Letters* **2019**, *15* (4), 481−492.
(89) Ben, L.; Yu, H.; Wu, Y.; Chen, B.; Zhao, W.; Huang, X. Ta2O5 Coating as an HF Barrier for Improving the Electrochemical Cycling Performance of High-Voltage Spinel LiNi0.5Mn1.5O4 at Elevated Temperatures. *ACS Applied Energy Materials* **2018**, *1* (10), 5589−5598.
(90) Chong, J.; Xun, S.; Song, X.; Liu, G.; Battaglia, V. S. Surface stabilized LiNi0.5Mn1.5O4 cathode materials with high-rate capa-

https://doi.org/10.1021/acsomega.3c09101
ACS Omega 2024, 9, 18688−18708

bility and long cycle life for lithium ion batteries. *Nano Energy* **2013**, *2* (2), 283−293.
(91) Yang, X.; Yang, T.; Liang, S.; Wu, X.; Zhang, H. Modification of LiNi0.5Mn1.5O4 high potential cathode from the inner lattice to the outer surface with Cr3+-doping and Li+-conductor coating. *Journal of Materials Chemistry A* **2014**, *2* (27), 10359−10364.
(92) Liu, D.; Trottier, J.; Charest, P.; Fréchette, J.; Guerfi, A.; Mauger, A.; Julien, C.; Zaghib, K. Effect of nano LiFePO4 coating on LiMn1.5Ni0.5O4 5 V cathode for lithium ion batteries. *J. Power Sources* **2012**, *204*, 127−132.
(93) Nisar, U.; Amin, R.; Essehli, R.; Shakoor, R. A.; Kahraman, R.; Kim, D. K.; Khaleel, M. A.; Belharouak, I. Extreme fast charging characteristics of zirconia modified LiNi0.5Mn1.5O4 cathode for lithium ion batteries. *J. Power Sources* **2018**, *396*, 774−781.
(94) Li, X.; Liu, J.; Banis, M. N.; Lushington, A.; Li, R.; Cai, M.; Sun, X. Atomic layer deposition of solid-state electrolyte coated cathode materials with superior high-voltage cycling behavior for lithium ion battery application. *Energy Environ. Sci.* **2014**, *7* (2), 768−778.
(95) George, S. M. Atomic Layer Deposition: An Overview. *Chem. Rev.* **2010**, *110* (1), 111−131.
(96) Cho, H.-M.; Chen, M. V.; MacRae, A. C.; Meng, Y. S. Effect of Surface Modification on Nano-Structured LiNi0.5Mn1.5O4 Spinel Materials. *ACS Appl. Mater. Interfaces* **2015**, *7* (30), 16231−16239.
(97) Song, J.; Han, X.; Gaskell, K.; Xu, K.; Lee, S.-B.; Hu, L. Enhanced electrochemical stability of high-voltage LiNi0.5Mn1.5O4 cathode by surface modification using atomic layer deposition. *J. Nanopart. Res.* **2014**, *16*, 2745.
(98) Xiao, B.; Liu, J.; Sun, Q.; Wang, B.; Banis, M. N.; Zhao, D.; Wang, Z.; Li, R.; Cui, X.; Sham, T.-K.; Sun, X. Unravelling the Role of Electrochemically Active FePO4 Coating by Atomic Layer Deposition for Increased High-Voltage Stability of LiNi0.5Mn1.5O4 Cathode Material. *Advanced Science* **2015**, *2* (5), 1500022.
(99) Deng, S.; Wang, B.; Yuan, Y.; Li, X.; Sun, Q.; Doyle-Davis, K.; Banis, M. N.; Liang, J.; Zhao, Y.; Li, J.; et al. Manipulation of an ionic and electronic conductive interface for highly-stable high-voltage cathodes. *Nano Energy* **2019**, *65*, 103988.
(100) Deng, S.; Xiao, B.; Wang, B.; Li, X.; Kaliyappan, K.; Zhao, Y.; Lushington, A.; Li, R.; Sham, T.-K.; Wang, H.; Sun, X. New insight into atomic-scale engineering of electrode surface for long-life and safe high voltage lithium ion cathodes. *Nano Energy* **2017**, *38*, 19−27.
(101) Park, J. S.; Meng, X.; Elam, J. W.; Hao, S.; Wolverton, C.; Kim, C.; Cabana, J. Ultrathin Lithium-Ion Conducting Coatings for Increased Interfacial Stability in High Voltage Lithium-Ion Batteries. *Chem. Mater.* **2014**, *26* (10), 3128−3134.
(102) Fang, X.; Ge, M.; Rong, J.; Che, Y.; Aroonyadet, N.; Wang, X.; Liu, Y.; Zhang, A.; Zhou, C. Ultrathin Surface Modification by Atomic Layer Deposition on High Voltage Cathode LiNi0.5Mn1.5O4 for Lithium Ion Batteries. *Energy Technology* **2014**, *2* (2), 159−165.
(103) Refly, S.; Floweri, O.; Mayangsari, T. R.; Sumboja, A.; Santosa, S. P.; Ogi, T.; Iskandar, F. Regeneration of LiNi1/3Co1/3Mn1/3O2 Cathode Active Materials from End-of-Life Lithium-Ion Batteries through Ascorbic Acid Leaching and Oxalic Acid Coprecipitation Processes. *ACS Sustainable Chem. Eng.* **2020**, *8* (43), 16104−16114.
(104) Hou, P.; Zhang, H.; Zi, Z.; Zhang, L.; Xu, X. Core-shell and concentration-gradient cathodes prepared via co-precipitation reaction for advanced lithium-ion batteries. *Journal of Materials Chemistry A* **2017**, *5* (9), 4254−4279.
(105) Dong, H.; Koenig, G. M. A review on synthesis and engineering of crystal precursors produced via coprecipitation for multicomponent lithium-ion battery cathode materials. *CrystEngComm* **2020**, *22* (9), 1514−1530.
(106) Qureshi, Z. A.; Tariq, H. A.; Hafiz, H. M.; Shakoor, R. A.; AlQaradawi, S.; Kahraman, R. Influence of graphene wrapped-cerium oxide coating on spherical LiNi0.5Mn1.5O4 particles as cathode in high-voltage lithium-ion batteries. *J. Alloys Compd.* **2022**, *920*, 165989.
(107) Wu, Z.-H.; Shih, J.-Y.; Li, Y.-J. J.; Tsai, Y.-D.; Hung, T.-F.; Karuppiah, C.; Jose, R.; Yang, C.-C. MoO3 Nanoparticle Coatings on High-Voltage 5 V LiNi0.5Mn1.5O4 Cathode Materials for Improving Lithium-Ion Battery Performance. *Nanomaterials* **2022**, *12* (3), 409.
(108) Luo, W.; Chao, Z.; Lu, S.; Liu, Y.; Fan, J. Effect of Thin Film to Boost the Electrochemical Properties of LiMn1.5Ni0.5O4. *Energy Fuels* **2021**, *35* (18), 15166−15171.
(109) Wu, H. M.; Belharouak, I.; Abouimrane, A.; Sun, Y. K.; Amine, K. Surface modification of LiNi0.5Mn1.5O4 by ZrP2O7 and ZrO2 for lithium-ion batteries. *J. Power Sources* **2010**, *195* (9), 2909−2913.
(110) Wang, G.; Wen, W.; Chen, S.; Yu, R.; Wang, X.; Yang, X. Improving the electrochemical performances of spherical LiNi0.5Mn1.5O4 by Fe2O3 surface coating for lithium-ion batteries. *Electrochim. Acta* **2016**, *212*, 791−799.
(111) Li, X.; Guo, W.; Liu, Y.; He, W.; Xiao, Z. Spinel LiNi0.5Mn1.5O4 as superior electrode materials for lithium-ion batteries: Ionic liquid assisted synthesis and the effect of CuO coating. *Electrochim. Acta* **2014**, *116*, 278−283.
(112) Deng, M.-M.; Tang, Z.-F.; Shao, Y.; He, X.-D.; Wen, Z.-Y.; Chen, C.-H. Enhancing the electrochemical performances of LiNi0.5Mn1.5O4 by Co3O4 surface coating. *J. Alloys Compd.* **2018**, *762*, 163−170.
(113) Xue, Y.; Zheng, L.-L.; Wang, J.; Zhou, J.-G.; Yu, F.-D.; Zhou, G.-J.; Wang, Z.-B. Improving Electrochemical Performance of High-Voltage Spinel LiNi0.5Mn1.5O4 Cathode by Cobalt Surface Modification. *ACS Applied Energy Materials* **2019**, *2* (4), 2982−2989.
(114) Wen, W.; Yang, X.; Wang, X.; Shu, L. G. H. Improved electrochemical performance of the spherical LiNi 0.5 Mn 1.5 O 4 particles modified by nano-Y 2 O 3 coating. *J. Solid State Electrochem.* **2015**, *19*, 1235.
(115) Pang, Q.; Fu, Q.; Wang, Y.; Zhang, Y.; Zou, B.; Du, F.; Chen, G.; Wei, Y. Improved Electrochemical Properties of Spinel LiNi0.5Mn1.5O4 Cathode Materials by Surface Modification with RuO2 Nanoparticles. *Electrochim. Acta* **2015**, *152*, 240−248.
(116) Xu, T.; Li, Y.; Wang, D.; Wu, M.; Pan, D.; Zhao, H.; Bai, Y. Enhanced Electrochemical Performance of LiNi0.5Mn1.5O4 Cathode Material by YPO4 Surface Modification. *ACS Sustainable Chem. Eng.* **2018**, *6* (5), 5818−5825.
(117) Yu, C.; Dong, L.; Zhang, Y.; Du, K.; Gao, M.; Zhao, H.; Bai, Y. Promoting electrochemical performances of LiNi0.5Mn1.5O4 cathode via YF3 surface coating. *Solid State Ionics* **2020**, *357*, 115464.
(118) Wu, Q.; Yin, Y.; Sun, S.; Zhang, X.; Wan, N.; Bai, Y. Novel AlF3 surface modified spinel LiMn1.5Ni0.5O4 for lithium-ion batteries: performance characterization and mechanism exploration. *Electrochim. Acta* **2015**, *158*, 73−80.
(119) Wu, Q.; Zhang, X.; Sun, S.; Wan, N.; Pan, D.; Bai, Y.; Zhu, H.; Hu, Y.-S.; Dai, S. Improved electrochemical performance of spinel LiMn1.5Ni0.5O4 through MgF2 nano-coating. *Nanoscale* **2015**, *7* (38), 15609−15617.
(120) Lee, T.; Kim, W.-K.; Lee, Y.; Ryou, M.-H.; Lee, Y. M. Effect of Al2O3 coatings prepared by RF sputtering on polyethylene separators for high-power lithium ion batteries. *Macromol. Res.* **2014**, *22* (11), 1190−1195.
(121) Sberveglieri, G.; Faglia, G.; Groppelli, S.; Nelli, P. Methods for the preparation of NO, NO2 and H2 sensors based on tin oxide thin films, grown by means of the r.f. magnetron sputtering technique. *Sens. Actuators, B* **1992**, *8* (1), 79−88.
(122) Asmatulu, R. 14 - Nanocoatings for corrosion protection of aerospace alloys. In *Corrosion Protection and Control Using Nanomaterials*, Saji, V. S., Cook, R., Eds.; Woodhead Publishing, 2012; pp 357−374.
(123) Rho, Y. H.; Kanamura, K.; Umegaki, T. LiCoO2 and LiMn2 O 4 Thin-Film Electrodes for Rechargeable Lithium Batteries: Preparation Using PVP Sol-Gel to Produce Excellent Electrochemical Properties. *J. Electrochem. Soc.* **2003**, *150* (1), A107.
(124) Matsushita, T.; Dokko, K.; Kanamura, K. Comparison of Electrochemical Behavior of LiCoO2 Thin Films Prepared by Sol-Gel and Sputtering Processes. *J. Electrochem. Soc.* **2005**, *152* (11), A2229.

https://doi.org/10.1021/acsomega.3c09101
ACS Omega 2024, 9, 18688−18708

(125) Ding, H.; Zhang, N.; Wang, P.; Dong, H.; Li, R.; Li, S. Role of carbon nanotube on preparation of spinel LiNi0.5Mn1.5O4 cathode. *J. Mater. Sci.* **2022**, *57* (30), 14440−14449.
(126) Xu, Y.-H.; Zhao, S.-X.; Deng, Y.-F.; Deng, H.; Nan, C.-W. Improved electrochemical performance of 5 V spinel LiNi0.5Mn1.5O4 microspheres by F-doping and Li4SiO4 coating. *Journal of Materiomics* **2016**, *2* (3), 265−272.
(127) Hao, X.; Bartlett, B. M. Improving the Electrochemical Stability of the High-Voltage Li-Ion Battery Cathode LiNi0.5Mn1.5O4 by Titanate-Based Surface Modification. *J. Electrochem. Soc.* **2013**, *160* (5), A3162.
(128) Zhao, G.; Lin, Y.; Zhou, T.; Lin, Y.; Huang, Y.; Huang, Z. Enhanced rate and high-temperature performance of La0.7Sr0.3MnO3-coated LiNi0.5Mn1.5O4 cathode materials for lithium ion battery. *J. Power Sources* **2012**, *215*, 63−68.
(129) Wei, A.; Li, W.; Zhang, L.; Liu, Z. Improved electrochemical performance of 5 V spinel LiNi 0.5 Mn 1.5 O 4 by La 2 O 3 surface coating for Li-ion batteries. *MATEC Web of Conferences* **2018**, *175*, 01030.
(130) Gao, J.; Yuan, T.; Luo, S.; Ruan, J.; Sun, H.; Yang, J.; Zheng, S. Boosting lithium ion storage of lithium nickel manganese oxide via conformally interfacial nanocoating. *J. Colloid Interface Sci.* **2020**, *570*, 153−162.
(131) Yi, T.-F.; Li, Y.-M.; Li, X.-Y.; Pan, J.-J.; Zhang, Q.; Zhu, Y.-R. Enhanced electrochemical property of FePO 4 -coated LiNi 0.5 Mn 1.5 O 4 as cathode materials for Li-ion battery. *Science Bulletin* **2017**, *62*, 1004.
(132) Lin, Y.; Yang, Y.; Yu, R.; Lai, H.; Huang, Z. Enhanced electrochemical performances of LiNi0.5Mn1.5O4 by surface modification with superconducting YBa2Cu3O7. *J. Power Sources* **2014**, *259*, 188−194.
(133) Zhu, Y.-R.; Yi, T.-F.; Zhu, R.-S.; Zhou, A.-N. Increased cycling stability of Li4Ti5O12-coated LiMn1.5Ni0.5O4 as cathode material for lithium-ion batteries. *Ceram. Int.* **2013**, *39*, 3087−3094.
(134) Deng, Y.; Mou, J.; He, L.; Xie, F.; Zheng, Q.; Xu, C.; Lin, D. A core-shell structured LiNi0.5Mn1.5O4@LiCoO2 cathode material with superior rate capability and cycling performance. *Dalton Transactions* **2018**, *47* (2), 367−375.
(135) Kim, H.; Byun, D.; Chang, W.; Jung, H.-G.; Choi, W. A nano-LiNbO3 coating layer and diffusion-induced surface control towards high-performance 5 V spinel cathodes for rechargeable batteries. *Journal of Materials Chemistry A* **2017**, *5* (47), 25077−25089.
(136) Wu, D.; Li, W.; Tegus, O.; Yang, Y.; Tian, X.; Bator, S. Solid Electrolyte Li1.4Al0.4Ti1.6(PO4)3 as Coating for High Voltage Spinel LiNi0.5Mn1.5O4 Cathode Material. *Int. J. Electrochem. Sci.* **2020**, *15* (5), 3715−3728.
(137) Kashyap, A.; Singh, N. K.; Soni, M.; Soni, A. Chapter 3 - Deposition of thin films by chemical solution-assisted techniques. In *Chemical Solution Synthesis for Materials Design and Thin Film Device Applications*, Das, S.; Dhara, S., Eds.; Elsevier, 2021; pp 79−117.
(138) Cushing, B. L.; Kolesnichenko, V. L.; O'Connor, C. J. Recent Advances in the Liquid-Phase Syntheses of Inorganic Nanoparticles. *Chem. Rev.* **2004**, *104* (9), 3893−3946.
(139) Alva, G.; Kim, C.; Yi, T.; Cook, J. B.; Xu, L.; Nolis, G. M.; Cabana, J. Surface Chemistry Consequences of Mg-Based Coatings on LiNi0.5Mn1.5O4 Electrode Materials upon Operation at High Voltage. *J. Phys. Chem. C* **2014**, *118* (20), 10596−10605.
(140) Xiong, L.; Long, Q.; Wang, Y.; Xiang, Y.; Wu, X.; He, Z. Sandwich-structured graphene sheets@LiNi0.5Mn1.5O4@graphene sheets composites as cathode materials for lithium ion batteries with high rate performance. *Ceram. Int.* **2016**, *42*, 14141.
(141) Alcántara, R.; Jaraba, M.; Lavela, P.; Tirado, J. L. X-ray diffraction and electrochemical impedance spectroscopy study of zinc coated LiNi0.5Mn1.5O4 electrodes. *J. Electroanal. Chem.* **2004**, *566* (1), 187−192.
(142) Zhao, J.; Liu, Y.; He, Y.; Lu, K. Li4Ti5O12 epitaxial coating on LiNi0.5Mn1.5O4 surface for improving the electrochemical performance through solvothermal-assisted processing. *J. Alloys Compd.* **2019**, *779*, 978−984.
(143) Tao, S.; Kong, F.; Wu, C.; Su, X.; Xiang, T.; Chen, S.; Hou, H.; Zhang, L.; Fang, Y.; Wang, Z.; et al. Nanoscale TiO2 membrane coating spinel LiNi0.5Mn1.5O4 cathode material for advanced lithium-ion batteries. *J. Alloys Compd.* **2017**, *705*, 413−419.
(144) Sun, Y. K.; Hong, K. J.; Prakash, J.; Amine, K. Electrochemical performance of nano-sized ZnO-coated LiNi0.5Mn1.5O4 spinel as 5 V materials at elevated temperatures. *Electrochem. Commun.* **2002**, *4* (4), 344−348.
(145) Yi, T.-F.; Han, X.; Chen, B.; Zhu, Y.-R.; Xie, Y. Porous sphere-like LiNi0.5Mn1.5O4-CeO2 composite with high cycling stability as cathode material for lithium-ion battery. *J. Alloys Compd.* **2017**, *703*, 103−113.
(146) Ma, F.; Geng, F.; Yuan, A.; Xu, J. Facile synthesis and characterization of a SnO2-modified LiNi0.5Mn1.5O4 high-voltage cathode material with superior electrochemical performance for lithium ion batteries. *Phys. Chem. Chem. Phys.* **2017**, *19* (15), 9983−9991.
(147) Deng, M.-m.; Zhang, D.-w.; Shao, Y.; He, X.-d.; Yasmin, A.; Chen, C.-h. Improving interfacial electrochemistry of LiNi0.5Mn1.5O4 cathode coated by Mn3O4. *Chinese Journal of Chemical Physics* **2020**, *33* (4), 485−490.
(148) Wang, J.; Yao, S.; Lin, W.; Wu, B.; He, X.; Li, J.; Zhao, J. Improving the electrochemical properties of high-voltage lithium nickel manganese oxide by surface coating with vanadium oxides for lithium ion batteries. *J. Power Sources* **2015**, *280*, 114−124.
(149) Guo, J.; Li, Y.; Chen, Y.; Deng, S.; Zhu, J.; Wang, S.; Zhang, J.; Chang, S.; Zhang, D.; Xi, X. Stable interface Co3O4-coated LiNi0.5Mn1.5O4 for lithium-ion batteries. *J. Alloys Compd.* **2019**, *811*, 152031.
(150) Li, Y.; Guo, J.; Chen, Y.; Deng, S.; Zhu, J.; Cao, G.; Lei, T.; Zhang, J.; Wang, S.; Chang, S. Phase transition regulation and Cd-O/Cd-F compounds multi-effect modification synergistically act on LiNi0.5Mn1.5O4 cathode. *Ionics* **2020**, *26*, 1681.
(151) Chang, Q.; Wei, A.; Li, W.; Bai, X.; Zhang, L.; He, R.; Liu, Z. Structural and electrochemical characteristics of Al2O3-modified LiNi0.5Mn1.5O4 cathode materials for lithium-ion batteries. *Ceram. Int.* **2019**, *45*, 5100.
(152) Fan, Y.; Wang, J.; Tang, Z.; He, W.; Zhang, J. Effects of the nanostructured SiO2 coating on the performance of LiNi0.5Mn1.5O4 cathode materials for high-voltage Li-ion batteries. *Electrochim. Acta* **2007**, *52* (11), 3870−3875.
(153) Pang, W. K.; Lin, H.-F.; Peterson, V. K.; Lu, C.-Z.; Liu, C.-E.; Liao, S.-C.; Chen, J.-M. Enhanced Rate-Capability and Cycling-Stability of 5 V SiO2- and Polyimide-Coated Cation Ordered LiNi0.5Mn1.5O4 Lithium-Ion Battery Positive Electrodes. *J. Phys. Chem. C* **2017**, *121* (7), 3680−3689.
(154) Jung, S.; Kim, D.; Brüner, P.; Lee, H.; Hah, H.; Kim, S.; Jung, Y. S. Extremely conductive RuO2-coated LiNi0.5Mn1.5O4 for lithium-ion batteries. *Electrochim. Acta* **2017**, *232*, 236.
(155) Han, Y.; Xue, Y.; Xia, Y.-F.; Zhang, J.-N.; Yu, F.-D.; Gu, D.-M.; Wang, Z.-B. Design of synergistic-coated layer of La2O3/Al2O3 in LiNi0.5Mn1.5O4 cathode for enhanced cycling stability and rate capability. *Ionics* **2019**, *25*, 2459.
(156) Yang, Y.; Li, S.; Zhang, Q.; Zhang, Y.; Xu, S. Spherical Agglomeration of Octahedral LiNi0.5Co4xMn1.5−3xO4 Cathode Material Prepared by a Continuous Coprecipitation Method for 5 V Lithium-Ion Batteries. *Ind. Eng. Chem. Res.* **2017**, *56* (1), 175−182.
(157) Wei, A.; Mu, J.; He, R.; Bai, X.; Liu, Z.; Zhang, L.; Wang, Y.; Liu, Z. Enhancing electrochemical performance and structural stability of LiNi0.5Mn1.5O4 cathode material for rechargeable lithium-ion batteries by boron doping. *Ceram. Int.* **2021**, *47* (1), 226−237.
(158) Liu, M.-H.; Huang, H.-T.; Lin, C.-M.; Chen, J.-M.; Liao, S.-C. Mg gradient-doped LiNi0.5Mn1.5O4 as the cathode material for Li-ion batteries. *Electrochim. Acta* **2014**, *120*, 133−139.
(159) Deng, Y.-F.; Zhao, S.-X.; Xu, Y.-H.; Gao, K.; Nan, C.-W. Impact of P-Doped in Spinel LiNi0.5Mn1.5O4 on Degree of Disorder, Grain Morphology, and Electrochemical Performance. *Chem. Mater.* **2015**, *27* (22), 7734−7742.

https://doi.org/10.1021/acsomega.3c09101
ACS Omega 2024, 9, 18688−18708

(160) Luo, Y.; Li, H.; Lu, T.; Zhang, Y.; Mao, S. S.; Liu, Z.; Wen, W.; Xie, J.; Yan, L. Fluorine gradient-doped LiNi0.5Mn1.5O4 spinel with improved high voltage stability for Li-ion batteries. *Electrochim. Acta* **2017**, *238*, 237−245.
(161) Lin, F.; Guo, J.; Wang, L.; Zhou, Y.; Wu, H.; Zhou, D. Synergistic effect of Mg and Y co-dopants on enhancement of electrochemical properties of LiNi0.5Mn1.5O4 spinel. *Electrochim. Acta* **2021**, *399*, 139433.
(162) Deng, J.; Xu, Y.; Xiong, L.; Li, L.; Sun, X.; Zhang, Y. Improving the fast discharge performance of high-voltage LiNi0.5Mn1.5O4 spinel by Cu2+, Al3+, Ti4+ tri-doping. *J. Alloys Compd.* **2016**, *677*, 18−26.
(163) Wang, S.; Li, P.; Shao, L.; Wu, K.; Lin, X.; Shui, M.; Long, N.; Wang, D.; Shu, J. Preparation of spinel LiNi0.5Mn1.5O4 and Cr-doped LiNi0.5Mn1.5O4 cathode materials by tartaric acid assisted sol-gel method. *Ceram. Int.* **2015**, *41* (1, Part B), 1347−1353.
(164) Kiziltas-Yavuz, N.; Yavuz, M.; Indris, S.; Bramnik, N.; Knapp, M.; Dolotko, O.; Das, B.; Ehrenberg, H.; Bhaskar, A. Enhancement of electrochemical performance by simultaneous substitution of Ni and Mn with Fe in Ni-Mn spinel cathodes for Li-ion batteries. *J. Power Sources* **2016**, *327*, 507−518.
(165) Luo, Y.; Lu, T.; Zhang, Y.; Yan, L.; Mao, S. S.; Xie, J. Surface-segregated, high-voltage spinel lithium-ion battery cathode material LiNi0.5Mn1.5O4 cathodes by aluminium doping with improved high-rate cyclability. *J. Alloys Compd.* **2017**, *703*, 289−297.
(166) Zong, B.; Deng, Z.; Yan, S.; Lang, Y.; Gong, J.; Guo, J.; Wang, L.; Liang, G. Effects of Si doping on structural and electrochemical performance of LiNi0.5Mn1.5O4 cathode materials for lithium-ion batteries. *Powder Technol.* **2020**, *364*, 725−737.
(167) Yi, T.-F.; Chen, B.; Zhu, Y.-R.; Li, X.-Y.; Zhu, R.-S. Enhanced rate performance of molybdenum-doped spinel LiNi0.5Mn1.5O4 cathode materials for lithium ion battery. *J. Power Sources* **2014**, *247*, 778−785.
(168) Zong, B.; Lang, Y.; Yan, S.; Deng, Z.; Gong, J.; Guo, J.; Wang, L.; Liang, G. Influence of Ti doping on microstructure and electrochemical performance of LiNi0.5Mn1.5O4 cathode material for lithium-ion batteries. *Materials Today Communications* **2020**, *24*, 101003.
(169) Feng, S.; Kong, X.; Sun, H.; Wang, B.; Luo, T.; Liu, G. Effect of Zr doping on LiNi0.5Mn1.5O4 with ordered or disordered structures. *J. Alloys Compd.* **2018**, *749*, 1009−1018.
(170) Wang, J.; Lin, W.; Wu, B.; Zhao, J. Syntheses and electrochemical properties of the Na-doped LiNi0.5Mn1.5O4 cathode materials for lithium-ion batteries. *Electrochim. Acta* **2014**, *145*, 245−253.
(171) Sun, H. Y.; Kong, X.; Wang, B. S.; Luo, T. B.; Liu, G. Y. Cu doped LiNi0.5Mn1.5-xCuxO4 (x = 0, 0.03, 0.05, 0.10, 0.15) with significant improved electrochemical performance prepared by a modified low temperature solution combustion synthesis method. *Ceram. Int.* **2018**, *44* (5), 4603−4610.
(172) Wu, W.; Guo, J.; Qin, X.; Bi, C.; Wang, J.; Wang, L.; Liang, G. Enhanced electrochemical performances of LiNi0.5Mn1.5O4 spinel in half-cell and full-cell via yttrium doping. *J. Alloys Compd.* **2017**, *721*, 721−730.
(173) Chae, J. S.; Jo, M. R.; Kim, Y.-I.; Han, D.-W.; Park, S.-M.; Kang, Y.-M.; Roh, K. C. Kinetic favorability of Ru-doped LiNi0.5Mn1.5O4 for high-power lithium-ion batteries. *Journal of Industrial and Engineering Chemistry* **2015**, *21*, 731−735.
(174) Sun, H.; Kong, X.; Wang, B.; Luo, T.; Liu, G. LiNi0.5Mn1.45Zn0.05O4 with Excellent Electrochemical Performance for Lithium Ion Batteries. *Int. J. Electrochem. Sci.* **2017**, *12* (9), 8609−8621.
(175) Kim, W.-K.; Han, D.-W.; Ryu, W.-H.; Lim, S.-J.; Eom, J.-Y.; Kwon, H.-S. Effects of Cl doping on the structural and electrochemical properties of high voltage LiMn1.5Ni0.5O4 cathode materials for Li-ion batteries. *J. Alloys Compd.* **2014**, *592*, 48−52.
(176) Li, S.; Wei, Y.; Wang, P.; Feng, Y.; Liang, W.; Ding, H.; Cui, X. Synergism of Cu and Al co-doping on improvements of structural integrity and electrochemical performance for LiNi0.5Mn1.5O4. *J. Alloys Compd.* **2020**, *820*, 153140.
(177) Shu, X.; Zhao, H.; Hu, Y.; Liu, J.; Tan, M.; Liu, S.; Zhang, M.; Ran, Q.; Li, H.; Liu, X. Magnesium and silicon co-doped LiNi0.5Mn1.5O4 cathode material with outstanding cycling stability for lithium-ion batteries. *Vacuum* **2018**, *156*, 1−8.
(178) Zheng, X.; Liu, W.; Qu, Q.; Zheng, H.; Huang, Y. Bi-functions of titanium and lanthanum co-doping to enhance the electrochemical performance of spinel LiNi0.5Mn1.5O4 cathode. *Journal of Materiomics* **2019**, *5* (2), 156−163.
(179) Wang, L.; Chen, D.; Wang, J.; Liu, G.; Wu, W.; Liang, G. Improved structural and electrochemical performances of LiNi0.5Mn1.5O4 cathode materials by Cr3+ and/or Ti4+ doping. *RSC Adv.* **2015**, *5* (121), 99856−99865.
(180) Duncan, H.; Duguay, D.; Abu-Lebdeh, Y.; Davidson, I. J. Study of the LiMn1.5Ni0.5O4/Electrolyte Interface at Room Temperature and 60°C. *J. Electrochem. Soc.* **2011**, *158* (5), A537.
(181) Strauss, E.; Golodnitsky, D.; Peled, E. Cathode Modification for Improved Performance of Rechargeable Lithium/Composite Polymer Electrolyte-Pyrite Battery. *Electrochem. Solid-State Lett.* **1999**, *2* (3), 115.
(182) Xie, Y.; Gao, H.; Gim, J.; Ngo, A. T.; Ma, Z.-F.; Chen, Z. Identifying Active Sites for Parasitic Reactions at the Cathode-Electrolyte Interface. *J. Phys. Chem. Lett.* **2019**, *10* (3), 589−594.
(183) Yin, Z.-W.; Peng, X.-X.; Li, J.-T.; Shen, C.-H.; Deng, Y.-P.; Wu, Z.-G.; Zhang, T.; Zhang, Q.-B.; Mo, Y.-X.; Wang, K.; et al. Revealing of the Activation Pathway and Cathode Electrolyte Interphase Evolution of Li-Rich 0.5Li2MnO3·0.5LiNi0.3Co0.3Mn0.4O2 Cathode by in Situ Electrochemical Quartz Crystal Microbalance. *ACS Appl. Mater. Interfaces* **2019**, *11* (17), 16214−16222.
(184) Lu, W.; Zhang, J.; Xu, J.; Wu, X.; Chen, L. In Situ Visualized Cathode Electrolyte Interphase on LiCoO2 in High Voltage Cycling. *ACS Appl. Mater. Interfaces* **2017**, *9* (22), 19313−19318.
(185) Yang, L.; Ravdel, B.; Lucht, B. L. Electrolyte Reactions with the Surface of High Voltage LiNi0.5Mn1.5O4 Cathodes for Lithium-Ion Batteries. *Electrochem. Solid-State Lett.* **2010**, *13* (8), A95.
(186) Li, Q.; Wang, Y.; Wang, X.; Sun, X.; Zhang, J.-N.; Yu, X.; Li, H. Investigations on the Fundamental Process of Cathode Electrolyte Interphase Formation and Evolution of High-Voltage Cathodes. *ACS Appl. Mater. Interfaces* **2020**, *12* (2), 2319−2326.
(187) Duncan, H.; Duguay, D.; Abu-Lebdeh, Y.; Davidson, I. Study of the LiMn1.5Ni0.5O4/Electrolyte Interface at Room Temperature and 60°C. *J. Electrochem. Soc.* **2011**, *158*, A537−A545.
(188) Cantor, B.; Chang, I.; Knight, P.; Vincent, A. Microstructural development in equiatomic multicomponent alloys. *Materials Science and Engineering: A* **2004**, *375*, 213−218.
(189) Zhang, R.; Wang, C.; Zou, P.; Lin, R.; Ma, L.; Yin, L.; Li, T.; Xu, W.; Jia, H.; Li, Q.; et al. Compositionally complex doping for zero-strain zero-cobalt layered cathodes. *Nature* **2022**, *610* (7930), 67−73.
(190) Ma, S.; Zou, P.; Xin, H. L. Extending phase-variation voltage zones in P2-type sodium cathodes through high-entropy doping for enhanced cycling stability and rate capability. *Materials Today Energy* **2023**, *38*, 101446.

https://doi.org/10.1021/acsomega.3c09101
ACS Omega 2024, 9, 18688−18708